Journal of the Geological Survey of Brazil vol 6, n2, 135 - 164, August 2023

Journal of the Geological Survey of Brazil

Stratigraphy of the Pitangui Synclinorium, northwest of the Quadrilátero Ferrífero mineral province - Brazil: magmatism and sedimentation from Archean to Neoproterozoic

Marcelo de Souza Marinho[1*], Joana Reis Magalhães[1], Julio Cesar Lombello[1], Joanna Chaves Souto Araújo[1], Luiz Paulo Pedrosa Di Salvio[1], Rosane Nascimento Silva[1], Denise Canabrava Brito[1], Wilson Luis Feboli[1], Camila Franco Basto[1]

[1]Geological Survey of Brazil (SGB-CPRM), Avenida Brasil, 1731 Belo Horizonte, MG, Brazil, CEP: 30140-002

Abstract

The Pitangui Synclinorium is located in the northwestern portion of the Quadrilátero Ferrífero mineral province, São Francisco Craton, in southeast Brazil. It corresponds to a NW-SE-trending synformal structure composed of an Archean greenstone belt sequence, which is covered by Paleoproterozoic metasedimentary rocks to Neoproterozoic sedimentary rocks, and surrounded by Archean granite-gneiss complexes. This study reports the first detailed 1:25.000 scale geological mapping in the Pitangui Synclinorium and provides cartographic, stratigraphic and petrographic improvements, allowing the formalization of its lithostratigraphic units and unraveling the sedimentary and volcanic depositional environments. The Archean Pitangui greenstone belt occurs in most parts of the homonymous synclinorium, and is subdivided into the Pitangui Group and the Antimes Formation. The metavolcano-sedimentary sequence of the Pitangui Group comprises basal mafic/ultramafic metavolcanic rocks with subordinate felsic/intermediate metavolcanic and metavolcaniclastic rocks of the Rio Pará Formation, suggesting a bimodal volcanism. It is followed by volcanogenic and chemical metasedimentary rocks of the Rio São João Formation, and pelitic to sandy metasedimentary rocks of the Onça do Pitangui Formation deposited in subaqueous environments mainly corresponding to submarine fan systems. The occurrence of clastic rocks increases towards the top of the sequence. The Antimes Formation comprises quartzites and metaconglomerates related to fluvial and fan delta depositional environments. The Pitangui greenstone belt is overlapped, in the central and northwest regions of the study area, by the Fazenda Tapera Formation, a Paleoproterozoic siliciclastic package containing arkosic metasandstones, metagreywackes and metarhythmites deposited in a shallow marine environment. Subordinated tuff layers occur as ash/fall deposits from distal volcanism. Neoproterozoic clastic-chemical sedimentary rocks of the Bambuí Group cover the northern portions of the synclinorium, and are mainly composed of diamictites, limestones, marls and rhythmites from the Carrancas (lacustrine or restricted marine), Sete Lagoas (shallow marine) and Serra de Santa Helena formations (deep water grading to prodelta and delta front).

Article Information

Publication type: Research Papers
Received 7 October 2022
Accepted 1 March 2023
Online pub. 6 March 2023
Editor: Evandro Klein

Keywords:
Greenstone belt
Volcanic associations
Rhyacian basin
Ediacaran sedimentation
São Francisco Craton

*Corresponding author
Marcelo de Souza Marinho
E-mail address: marcelo.marinho@sgb.gov.br

1. Introduction

The rock stratigraphic record is a fundamental puzzle to unravel the geological history of any terrain, tracking diverse processes on Earth, such as basin subsidence, sea-level fluctuations, volcanism and climate change, among others (e.g., Eriksson et al. 1994; Eriksson et al. 2004 and references therein). Therefore, it is a powerful and imperative indicator for defining depositional and tectonic environments.

Stacking a stratigraphic succession is especially challenging in metamorphosed and polydeformed terrains, as lithological sections can be thinned, thickened, partially or entirely removed by tectonic processes and plutonism (Condie 1981). Furthermore, the reconstruction of the stratigraphic record may be hampered by climate, regolith cover and bio-influence (Straub et al. 2020).

The Pitangui Synclinorium, located at the southern edge of the São Francisco craton, SE Brazil (Figure 1), comprises an Archean greenstone belt sequence, Paleoproterozoic metasedimentary rocks and Neoproterozoic clastic-chemical rocks (Romano 2007; Marinho et al. 2019; Brando-Soares et al. 2020). It is a NW-SE-trending

ISSN: 2595-1939
https://doi.org/10.29396/jgsb.2023.v6.n2.1
Open access at jgsb.cprm.gov.br

synformal structure bordered by Archean granite-gneiss complexes in the northwestern portion of the Quadrilátero Ferrífero (QF, 'Iron Quadrangle') mineral province (Dorr 1969; Lobato et al. 2001).

This megastructure hosts important gold deposits such as Turmalina, Satinoco, and São Sebastião deposits (Figure 2; Brando-Soares et al. 2018; Fabricio-Silva et al. 2019 and references therein). In addition, the region has several and relevant agalmatolite deposits, which represent pyrophyllite-rich products of hydrothermal alteration of felsic volcanic rocks (e.g., Carmo and Romano 1996; Romano 2007). However, despite its metallogenic potential and previous studies (Romano and Carmo 1992; Romano 2007; Brando-Soares et al. 2020; Melo-Silva et al. 2020 and others), much remains to be done with regard to the stratigraphic and structural evolution of the Pitangui Synclinorium.

In this contribution, we present a cartographic refinement of the Pitangui Synclinorium based on 12 geological maps at 1:25,000 scale (Brito et al. 2019a, 2019b; Brito and Marinho 2019; Di Salvio et al. 2019a, 2019b, 2019c; Féboli and Marinho 2019a, 2019b; Féboli et al. 2019; Lombello and Marinho 2019a, 2019b, 2019c; Figure 1B), an integration map at 1:75,000 scale (Marinho et al. 2019 - Figure 2), field and petrographic databases (CPRM 2019) and preliminary geochronological data obtained by the Geological Survey of Brazil (Di Salvio et al. 2017; Marinho et al. 2017; Brito et al. 2018; Magalhães et al. 2019). We provide an overview of the informal nomenclature of its lithostratigraphic units and set out a formal classification and terminology for the volcano-sedimentary units (Figures 2 and 3), which are described in detail in the following sections. Finally, we present depositional models for the stratigraphic record.

2. Geological context

The southern region of the São Francisco Craton, in which the Pitangui Synclinorium is located (Figure 1), is composed of Meso- to Neoarchean complexes represented by TTG (tonalite-trondhjemite-granodiorite) gneisses and migmatites, Neoarchean medium- and high-K granitoids, and Meso- to Neoarchean greenstones belts covered by Proterozoic supracrustal rocks (Machado et al. 1996; Alkmim and Marshak 1998; Romano 2007; Lana et al. 2013; Romano et al. 2013; Farina et al. 2015, 2016; Brando-Soares et al. 2017; Araújo et al. 2020).

Several tectono-magmatic events are recognized in the study area (Lana et al. 2013; Farina et al. 2015, 2016; Teixeira et al. 2015) using zircon U-Pb geochronology: Rio das Velhas I (2.93–2.85 Ga), Rio das Velhas II (2.80–2.76 Ga), Mamona I (2.75–2.68 Ga), Mamona II (2.62–2.58 Ga), and Minas Orogeny (2.50-2.00 Ga).

The Belo Horizonte and Divinópolis complexes outline the Pitangui Synclinorium to the northeast and southwest, respectively (Figure 2), through sinistral transpressional shear zones (Marinho et al. 2019). These complexes are predominantly composed of gneissic rocks with a chemical composition similar to Archean TTGs (Noce et al. 1997). U-Pb zircon data for these gneisses indicate crystallization ages from 2.91 to 2.76 Ga, with inherited age of 3.20 Ga, and migmatization and metamorphism between 2.76 to 2.63 Ga (Noce et al. 1998; Lana et al. 2013; Farina et al. 2015; Martins et al. 2022). Intrusive granitoids, apparently derived from reworking of the TTG crust during the Neoarchean, have U-Pb zircon ages ranging from 2.78 to 2.60 Ga (Carneiro 1992; Noce 1995; Lana et al. 2013; Romano et al. 2013; Farina et al. 2015; Martins et al. 2022).

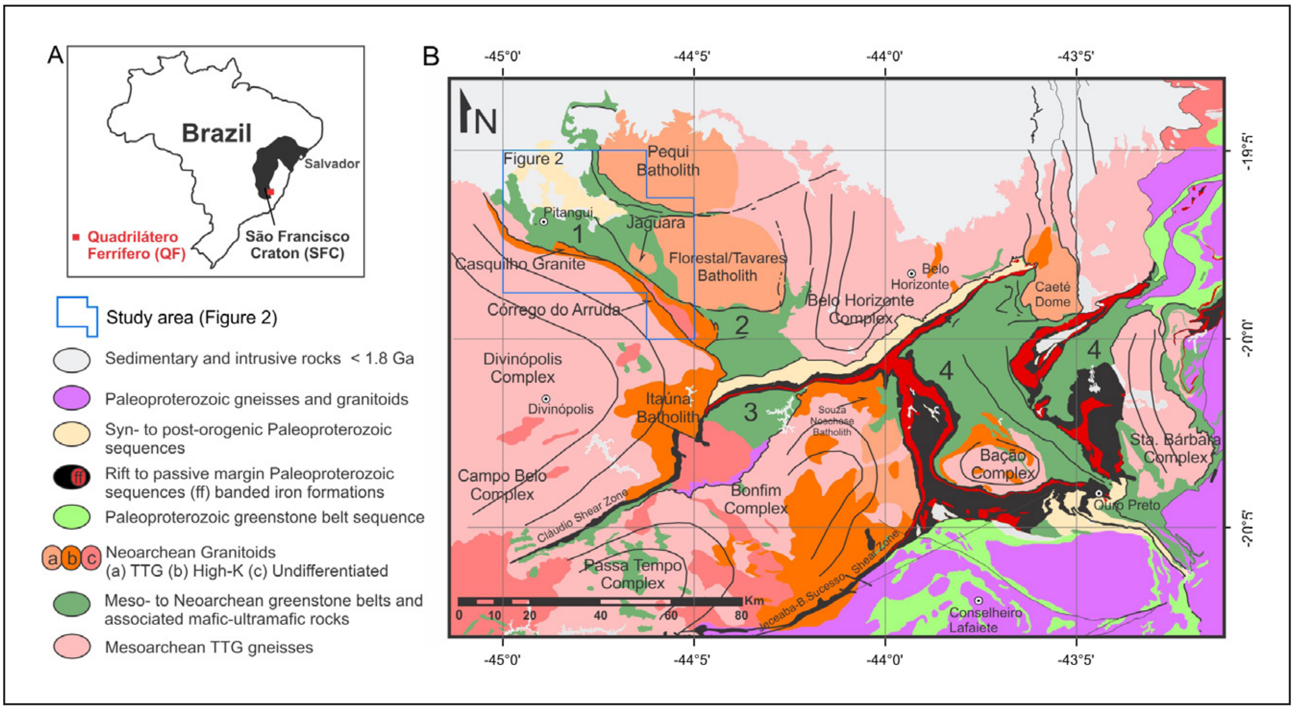

FIGURE 1. A) Location of the Pitangui Synclinorium in the southeastern border of the São Francisco craton, southeastern Brazil. B) Simplified geological map of the Quadrilátero Ferrífero (QF) mineral province highlighting Archean greenstone belts (1- Pitangui, 2- Mateus Leme, 3- Souzas, and 4- Rio das Velhas), TTG gneisses, Neoarchean granitoids and Paleoproterozoic units. Modified from Silva et al. (2020).

Bordering the Pitangui Synclinorium, the Neoarchean medium-K magmatism is represented by the Maravilhas-Florestal Suite (Pequi, Serra dos Tavares and Jaguara plutons; Figure 2) dated at approximately 2.76 Ga (U-Pb LA-ICPMS zircon dating; e.g., Romano et al. 2013; Brando-Soares et al. 2020). The high-K magmatism includes the Córrego do Arruda and Casquilho granites (Figure 2), with ages of 2.77 and 2.71 Ga, respectively (U-Pb LA-ICPMS zircon dating; Magalhães et al. 2019; Marinho et al. 2019).

The majority of previous studies on the Pitangui Synclinorium proposed a stratigraphy composed of an Archean greenstone belt covered by Neoproterozoic sedimentary rocks. Before the present work, only informal stratigraphic subdivisions of the Archean Pitangui greenstone belt (PGB; Brando-Soares et al. 2017) were available. The first studies presented by Grossi-Sad (1968) and Costa and Romano (1976) correlated Archean supracrustal rocks to other Archean greenstone belt sequence located in the central portion of the Quadrilátero Ferrífero mineral province, named Rio das Velhas greenstone belt (RVGB, Figure 1). Romano (1989) associated the basal portion of the PGB with the Nova Lima Group, which comprises the basal and intermediate rocks of the RVGB. Posteriorly, Romano (2007) divided these basal rocks into two sequences: lower (metaigneous and metasedimentary), and upper (metavolcano-sedimentary and metasedimentary). The quartzites and metaconglomerates overlying the Nova Lima Group were correlated with the Maquiné Group of the RVGB. Alternatively, Frizzo et al. (1991) inserted the basal metavolcano-sedimentary rocks in the Pitangui Group, and associated the upper metasedimentary lithologies to the Neoarchean-Siderian Minas Supergroup (2.65-2.33 Ga; Machado et al. 1996; Schrank and Machado 1996; Hartmann et al. 2006; Koglin et al. 2014; Dopico et al. 2017; Rossignol et al. 2020).

Recently, Brando-Soares et al. (2017) divided the Pitangui greenstone belt (PGB) into three informal units: lower, intermediate and upper. The lower unit consists of mafic metavolcanic rocks represented by metabasalts, komatiitic metabasalts and metaultramafic rocks, with intercalations of banded iron formations (BIFs), metacherts and carbonaceous phyllites. The intermediate unit is composed of rhythmic clastic metasedimentary rocks intercalated with intermediate metavolcanic rocks, and subordinate metabasalts. The upper unit is predominantly composed of clastic sedimentary rocks. Marinho et al. (2017) also subdivided the greenstone belt sequence into three informal units, defined by their predominant lithological associations: i) basal unit: mafic to intermediate metavolcanic rocks with subordinate metaultramafic, chemical and clastic metasedimentary rocks; ii) intermediate unit: mainly composed of metarhythmites (metapelite-metagraywacke-metaconglomerate association), with intercalations of BIFs; and iii) upper unit: quartzites, conglomeratic quartzites, metaconglomerates and rare sericitic phyllites.

U-Pb LA-ICPMS zircon geochronological data available for the basal unit revealed a maximum depositional age of 2877 ± 4 Ma for metaignimbrite layers (Di Salvio et al. 2017) and a crystallization age of 2740 ± 12 Ma for a tholeiitic metabasalt (Melo-Silva et al. 2020). Maximum depositional ages of 2859 ± 11 Ma (Brando-Soares et al. 2017) and 2770 ± 9 Ma (Melo-Silva et al. 2020) are also available for a meta-arenite and a metapelite interlayered in the basal unit, respectively. For the intermediate unit, detrital zircon grains from metagreywackes provided a maximum depositional age of 2.79 Ga (U-Pb, Marinho et al. 2017). For the upper unit, Marinho et al. (2017) and Brando-Soares et al. (2020) present zircon U-Pb maximum depositional ages of 2.69 Ga and 2812 ± 13 Ma, respectively, from metaconglomerates.

The PGB is interpreted as an ocean basin developed in a collisional zone between two continental blocks, namely the Divinópolis and Belo Horizonte complexes, along the Pitangui lineament (Romano and Paiva 1997). According to Melo-Silva et al. (2020) and Verma et al. (2017), the PGB basalts have a MORB (mid-ocean ridge basalts) signature and the greenstone belt is related to an active continental margin setting. Based on geochemical data, Brando Soares et al. (2020) propose that the PGB developed in a back-arc rift under a thick lithosphere, associated with an oceanic island arc, with subsequent collision.

The Neoproterozoic sedimentary rocks that cover the Archean Pitangui greenstone belt belong to the Bambuí Group (Reis et al. 2017; Matos et al. 2022). This unit is composed of shales, carbonate rocks, sandstones and subordinate coarse siliciclastic rocks (Dardenne 1978, 1981). From bottom to top, this group is represented by transgressive glaciogenic strata and associated deposits of the Carrancas Formation (Rocha-Campos et al. 2011; Kuchenbecker et al. 2013), followed by the regressive carbonate succession of the Sete Lagoas Formation (Vieira et al. 2007; Martins and Lemos 2007). These rocks are covered by the siliciclastic-carbonate sequences of the Serra de Santa Helena, Lagoa do Jacaré and Serra da Saudade formations that grade into tempestites and sandstones of the Três Marias Formation (Martins and Lemos 2007).

The geochronological dataset of the Bambuí Group has expanded in the last decade. Detrital zircon from marls of the basal Sete Lagoas Formation yielded a maximum depositional age (LA-ICPMS) of 593 ± 2 Ma (Paula-Santos et al. 2015). Dating calcite crystals (U-Pb LA-ICPMS) from limestones also of the Sete Lagoas Formation, Caxito et al. (2021) obtained ages of 615 ± 6 Ma, 608 ± 5 Ma and 607 ± 6 Ma for the base of this formation, and ages of 573 ± 11 Ma, 569 ± 7 Ma and 566 ± 15 Ma for the upper portion, correlating them to the post-Marinoan glaciation event. Furthermore, the recognition of the *Cloudina* fossil guide in the intermediate portion of the Sete Lagoas Formation certifies an Ediacaran age for this unit (Warren et al. 2014). For the upper part of the Bambuí Group, zircon grains from a tuff layer of the Serra da Saudade Formation revealed a maximum depositional age of 520 ± 5 (Moreira et al. 2020). For the Três Marias Formation, detrital zircon grains from a basal conglomerate suggest a 555 ± 17 Ma (U-Pb LA-ICPMS) maximum depositional age (Rossi et al. 2020), while a sandstone from the upper section revealed a maximum depositional age of 527 ± 4 Ma (U-Pb LA-ICPMS, Tavares et al. 2020).

3. Methods

This manuscript is part of the ‘Quadrilátero Ferrífero’ project from the Geological Survey of Brazil and encompasses the detailed 1:25.000 scale geological mapping of 12 geological map sheets in the northwest region of the QF, focusing on the Pitangui Synclinorium. The geological mapping activities involved a preparatory stage, with the

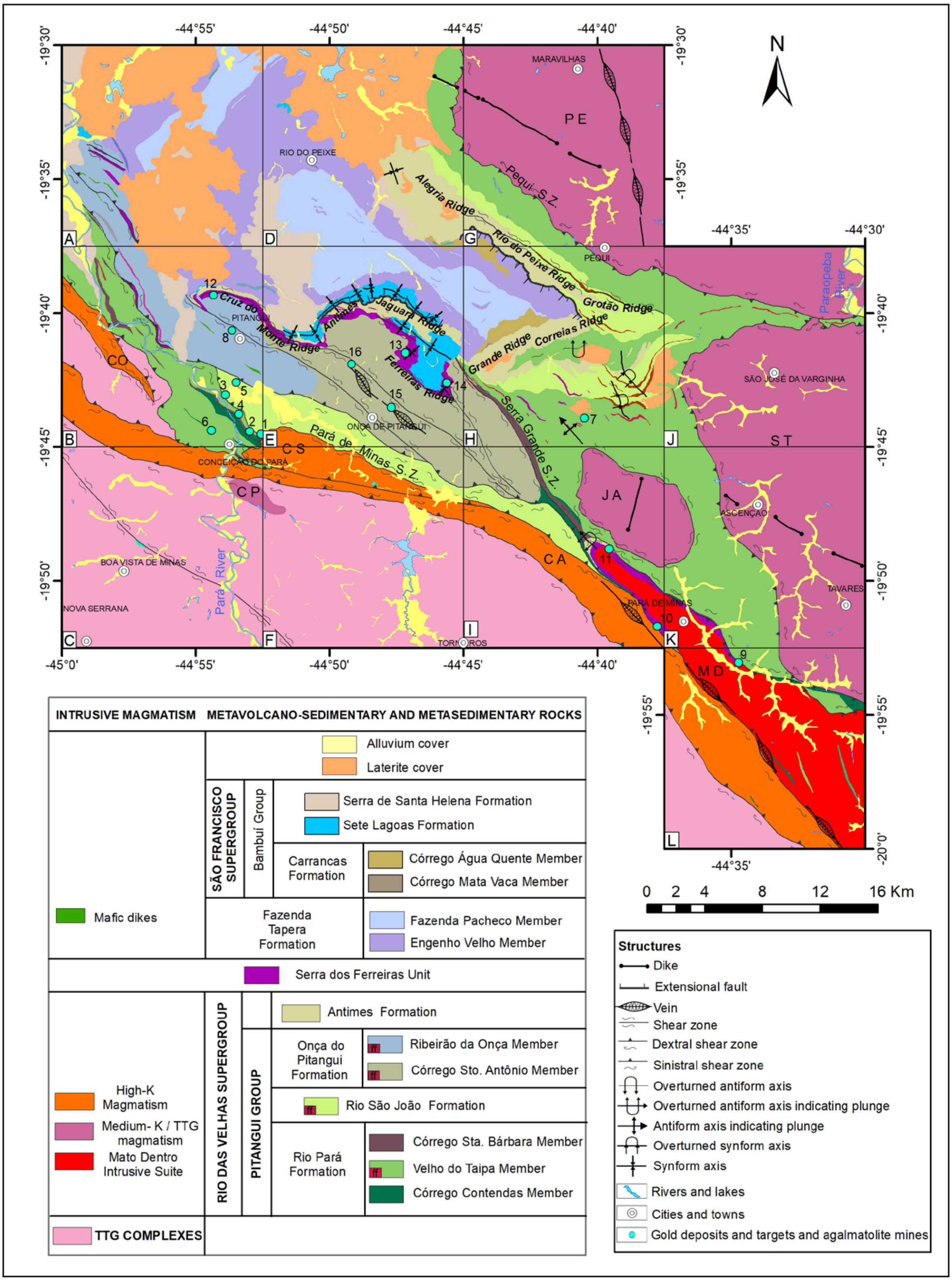

FIGURE 2. Simplified geological map of the Pitangui greenstone belt. ST: Serra dos Tavares Batholith, PE: Pequi Batholith, JA: Jaguara Pluton, CP: Conceição do Pará Pluton, CS: Casquilho Granite, CA: Córrego do Arruda Granite, CO: Coqueiro Granite, MD: Mato Dentro Suite, SZ: shear zone. Gold deposits: Turmalina (1), Satinoco (2), Pontal (3), Faina (4) and São Sebastião (7). Gold targets: Fazenda Experimental (5), Zona Basal (6), Penha district (8), Fazenda Santa Cruz (15) and Caxingó Sul (16). Agalmatolite mines: Pará de Minas (9), Córrego do Arroz (10), Capão Grosso/Praxedes (11), Córrego Seco (12), Fazenda Matão (13), and Serra dos Ferreiras (14). Modified from the 1:25,000 geological maps as follows: A - SE.23-Z-C-IV-1-NO (Di Salvio et al. 2019a); B - SE.23-Z-C-IV-1-SO (Di Salvio et al. 2019b); C - SE.23-Z-C-IV-3-NO (Di Salvio et al. 2019c); D - SE.23-Z-C-IV-1-NE (Brito et al. 2019a); E - SE.23-Z-C-IV-1-SE (Brito et al. 2019b); F - SE.23-Z-C-IV-3-NE, (Brito and Marinho 2019); G - SE.23-Z-C-IV-2-NO, (Féboli and Marinho 2019a); H - SE.23-Z-C-IV-2-SO (Féboli and Marinho 2019b), I - SE.23-Z-C-IV-4-NO (Féboli et al. 2019); J - SE.23-Z-C-IV-2-SE (Lombello and Marinho 2019a); K - SE.23-Z-C-IV-4-NE (Lombello and Marinho 2019b); L - SE.23-Z-C-IV-4-SE (Lombello and Marinho 2019c).

compilation of previous maps and published studies, and the interpretation of aerial photos, satellite images and airborne geophysical data (gamma spectrometry and magnetometry). During the fieldwork stages, geological profiles were made preferably transversal to the structures and geological units. The description of the outcrops (CPRM 2019) emphasized lithological, structural, magmatic, sedimentological and stratigraphic aspects. Unaltered or slightly weathered samples were selected for petrographic analyses, which were carried out using an Olympus BX51 transmitted and reflected light optical microscope, emphasizing the identification of protoliths and metamorphic, hydrothermal and deformational aspects.

To complement the few geochronological constraints available in the literature, preliminary U-Pb geochronological results (Di Salvio et al. 2017; Marinho et al. 2017; Brito et al. 2018; Magalhães et al. 2019) are presented to provide first-order time constraints for the stratigraphic units of Pitangui Synclinorium.

4. Stratigraphy of the Pitangui Synclinorium

The detailed 1:25,000 scale geological mapping accomplished in this work brought advances in the understanding of the stratigraphy of the Pitangui Synclinorium, allowing the formalization of its lithostratigraphic units that will be present in this section. Additionally, geochronological data obtained in this study revealed a Rhyacian (maximum depositional age of 2132 ± 13 Ma, Brito et al. 2018) unit inserted in this synclinorium.

The proposed stratigraphy of the Pitangui Synclinorium includes an Archean metavolcano-sedimentary sequence (Pitangui greenstone belt) composed of the Pitangui Group and the Antimes Formation, belonging to the Rio das Velhas Supergroup (Figures 2 and 3). The Serra dos Ferreiras informal unit, characterized by hydrothermally altered rocks, occurs associated with different rocks of the greenstone belt formations and, therefore, does not have a defined stratigraphic position.

These units are overlapped by Rhyacian (Brito et al. 2018) clastic metasedimentary rocks of the Fazenda Tapera Formation. Neoproterozoic clastic-chemical sedimentary rocks of the Bambuí Group cover all the succession.

The synclinorium structure has a NW-SE trend and is approximately 20 km wide and 50 km long. At the NE and SW, it is bordered by Archean granite-gneissic complexes, along the Pequi and Pará de Minas shear zones, respectively (Figures 1 and 2). Its eastern limit is marked by a Neoarchean granitic dome (Florestal Batholith) and its southeast continuity is represented by the Mateus Leme and Souzas synclinoriums. At its northern limit, the Pitangui Synclinorium deflects in a N-S trend under Bambuí Group cover (Matos et al. 2022).

4.1 Pitangui greenstone belt

4.1.1 Pitangui Group

The Pitangui Group represents the lowermost stratigraphic unit of the Archean metavolcano-sedimentary sequence and the main unit of the Pitangui Synclinorium. It comprises three formations, from base to top: Rio Pará, Rio São João and Onça do Pitangui (Figure 3).

This group crops out with a NW-SE trend, extending from the surroundings of the cities of Pará de Minas, Pitangui and Onça do Pitangui to the Pará and Paraopeba rivers (Figure 2). The metavolcano-sedimentary rocks of the Pitangui region were first named Pitangui Group by Frizzo et al. (1991), and represent a greenstone belt sequence.

The Pitangui Group shows tectonic contacts with Neoarchean granites of the Divinópolis and Belo Horizonte complexes (e.g., Jaguara, Pequi, Serra do Tavares, Florestal, Casquilho and Córrego do Arruda, Figure 1) (e.g., Romano 2007; Marinho et al. 2019). This group is covered by the Antimes Formation.

4.1.1.1 Rio Pará Formation

We formally propose the Rio Pará Formation to enclose the basal rocks of the Pitangui Group. This formation is the most important and largely distributed unit, hosting important gold deposits and occurrences of the Pitangui Synclinorium (such as Satinoco and São Sebastião; Frizzo et al. 1991; Brando-Soares et al. 2018; Fabrício-Silva et al. 2019). It occurs as NW-SE elongated strips, to the northeast, southwest and southeast of the Pitangui Synclinorium (Figure 2). The southwestern limb shows moderate to accentuated dip towards NE, while the northeastern limb presents moderate to accentuated dip towards SW.

The Rio Pará Formation shows tectonic contacts with gneisses and granitoids of the Divinópolis Complex, marked by transpressional shear zones. The contact with the Rio São João Formation (overlapping unit) is transitional, with a gradual increase in clastic-chemical metasedimentary rocks. In the western sector of the Pitangui Synclinorium, the contact with the Onça do Pitangui Formation is characterized by transpressional shear zones, while, in the central-eastern region, the Antimes Formation overlaps the Rio Pará Formation through an angular unconformity. In the central and northwestern areas, the Archean Rio Pará Formation is separated from the Rhyacian and Neoproterozoic sedimentary rocks of Fazenda Tapera Formation and Bambuí Group, respectively, by erosive/angular unconformities.

The Rio Pará Formation comprises the Córrego Contendas, Velho do Taipa and Córrego Santa Bárbara members (Figure 3), which occur interlayered. The stratigraphic relationships between them are marked by wide vertical and lateral lithological variations.

4.1.1.1.1 Córrego Contendas Member

The Córrego Contendas Member is mainly composed of metaultramafic rocks with subordinate metamafic rocks. Clastic-chemical metasedimentary rocks are rare, being represented by metapelites, metacherts and ferruginous metacherts. It is preferably arranged in a NW-SE to E-W trend (Figure 2) and crops out as lenses and layers of approximately 200 to 500 m width, reaching up to 700 m at the Córrego Contendas region, which is its type-area (quadrangle SE.23-Z-C-IV-4-SE, Lombello and Marinho 2019c).

The metaultramafic rocks are commonly represented by talc schists, with varying degrees of weathering. Primary features, such as pillow lobes, are rare. The main ultramafic rocks are (magnetite)-talc schists, (anthophyllite)-chlorite-talc schists, serpentine-talc-amphibole schists and serpentine-talc-magnetite-tremolite-chlorite fels (Figure 4A). They are usually composed of a groundmass of talc, serpentine and acicular tremolite, with aggregates of chlorite and tremolite in a decussate texture (Figure 4B, C). Pre-metamorphic texture is still partially preserved and mainly evidence 0.3 to 1-2 mm cumulates in a granular arrangement, replaced by ferromagnesian minerals. Schists may present mylonitic foliation (Figure 4D), crenulation cleavages (Figure 4E) and microscopic folds (Figure 4F). The presence of anthophyllite remnants may indicate that these rocks have reached the upper greenschist/amphibolite facies.

The metamafic rocks are mainly characterized by fine-grained plagioclase-amphibole schists composed of actinolite, plagioclase, chlorite, epidote, quartz, opaque minerals and some carbonate. Plagioclase crystals usually have skeletal shapes and amphibole can form radial aggregates. When present, carbonate is a product of hydrothermal alteration. The metamafic rocks may also present amygdales filled by quartz and chlorite and bordered by an actinolite fringe with crystals perpendicular to the rims.

4.1.1.1.2 Velho do Taipa Member

The Velho do Taipa Member is represented by large NW-SE trending layers on the limbs of the Pitangui Synclinorium, being the most expressive unit of the Pitangui Group (Figure 2). It reaches 1500 m thick and occurs in two main areas: (i) the southwest region of the synclinorium, west of the Velho do Taipa locality, near the Pará river, where the type-area is located

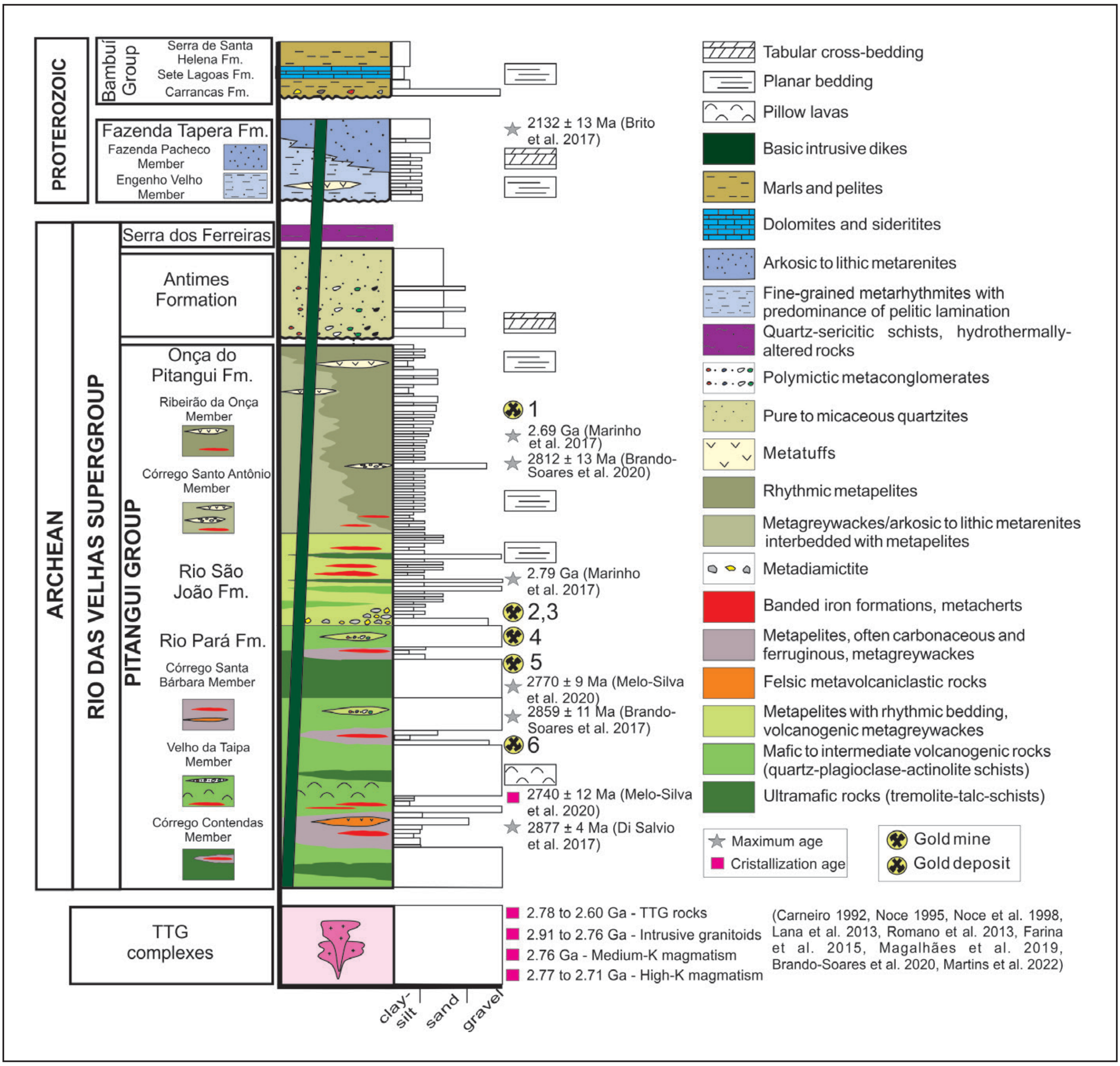

FIGURE 3. Stratigraphic column of the Pitangui Synclinorium. The figure does not represent the thickness of the layers. Gold mines and deposits: 1 – Trend Penha-Onça, 2 – Tourmaline complex, 3 – Pontal, 4 - Faina, 5 – Satinoco, and 6 - São Sebastião.

(quadrangle SE.23-Z-C-IV-1-SO, Di Salvio et al. 2019b); (ii) in the northeastern flank of the synclinal (quadrangles SE.23-Z-C-IV-1-NE, SE.23-Z-C-IV-2-NO, SE.23-Z-C-IV-2-SO, SE.23-Z-C-IV-4-NO, SE.23-Z-C-IV-2-SE, SE.23-Z-C-IV-4-NE and SE.23-Z-C-IV-4-SE, respectively, Brito et al. 2019a; Féboli and Marinho 2019a, 2019b; Féboli et al. 2019; Lombello and Marinho 2019a, 2019b, 2019c).

This member mainly comprises mafic metavolcanic rocks, which are associated with rare intermediate metavolcanic lithologies and metaultramafic rocks. Clastic-chemical metasedimentary rocks occur interlayered.

The metamafic rocks are aphanitic to fine-grained rocks (Figure 5A) represented by schists with actinolite, chlorite, plagioclase and variable amounts of quartz and epidote, defining plagioclase-chlorite schist, chlorite-actinolite-plagioclase schist, plagioclase-actinolite schist or fels. Generally, chlorite and amphibole are the main components of the rock groundmass, and may encompass granular

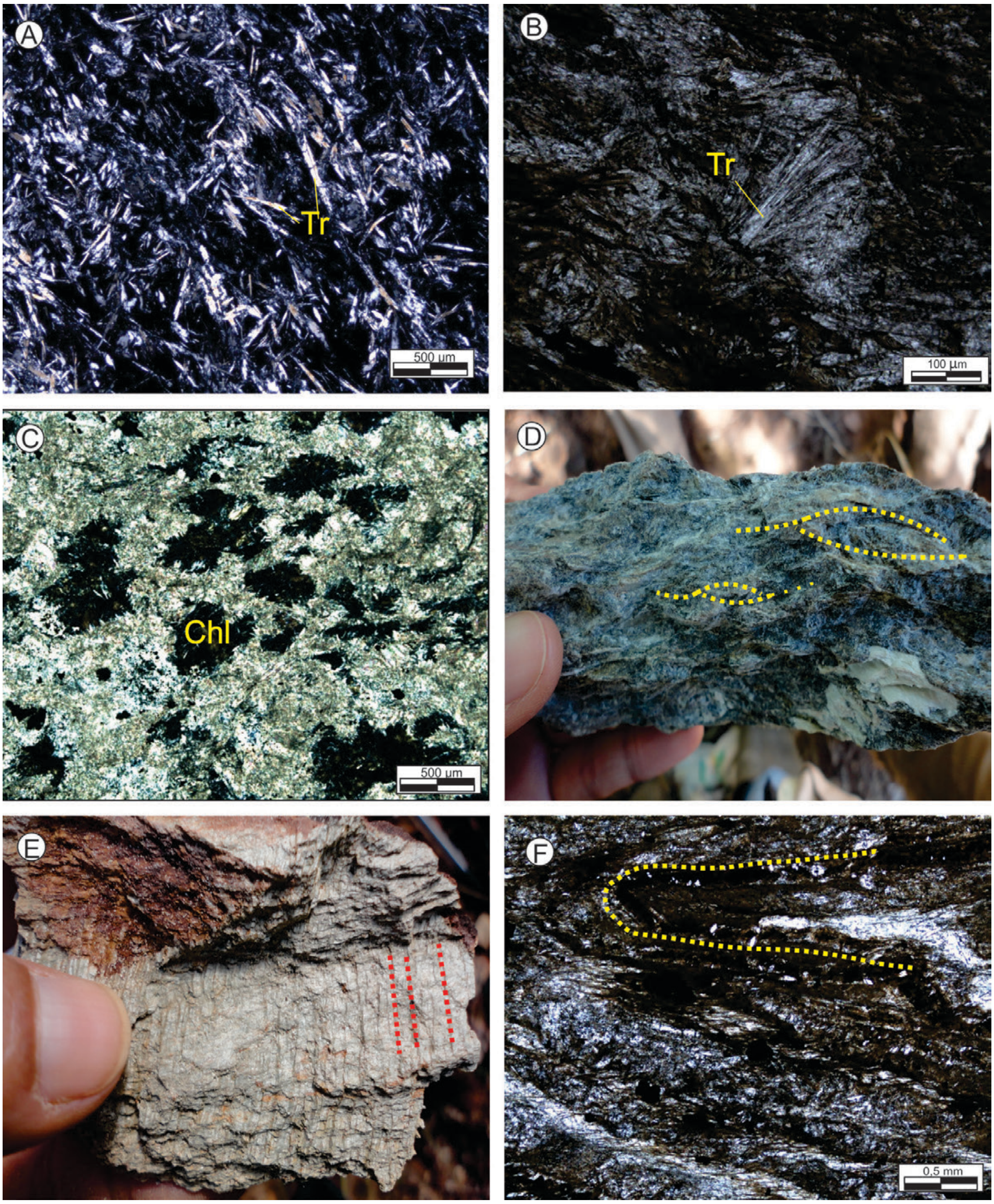

FIGURE 4. Córrego Contendas Member metaultramafic rocks. A) Thin-section of tremolite-chlorite-serpentine schist showing tremolite crystals with decussate texture (cross-polarized light, CPL); B) Photomicrography of tremolite pseudomorphs replaced by talc in a chlorite-talc schist (plane-polarized light, PPL); C) Photomicrography of a thin-section composed of acicular tremolite, talc and serpentine groundmass with chlorite aggregates (PPL); D) Hand sample of serpentine-talc-amphibole schist showing mylonitic foliation (dashed lines); E) Hand sample of talc schist evidencing a crenulation cleavage marked by the dashed lines; F) Photomicrography of a microscopic tight fold (dashed line) in chlorite-amphibole shale (PPL). Abbreviations: Tr = tremolite, Chl = chlorite.

plagioclase and amphibole phenocrysts up to 2 mm (Figure 5B, C). Minor phases include sphene, rutile, sericite, pyrite, tourmaline, apatite and/or carbonate. Mineral paragenesis indicates metamorphic conditions consistent with greenschist facies. Millimetric quartz veins are commonly observed. These rocks may show variolitic textures, forming rounded fibro-radiated aggregates of amphibole and plagioclase needles (Figure 5D), pointing to quench-induced crystallization.

When present, vesicular cavities are rounded, reaching up to 1 mm in diameter, and filled with amphibole, chlorite, epidote, quartz and/or sulfide. Peperite also occurs. In the Pará river, western region of the area (Figure 2), Ladeira (1981) first characterized variolitic metabasalts with pillow lava structures and chemical metasedimentary rocks, indicating their subaqueous origin (Figure 5E).

Intermediate rocks invariably occur weathered, and their best exposures are located along an inactive railroad, in the western region of Pará de Minas. These lithologies are characterized by an aphanitic to fine-grained, yellowish to reddish groundmass involving fine kaolinized phenocrysts of K-feldspar. The felsic-intermediate metavolcanic rocks are classified as metadacites and meta-andesites by Brando-Soares et al. (2017).

Chemical metasedimentary rocks interlayering the mafic metavolcanics correspond to centimetric to decametric lenses and layers of BIFs, ferruginous and pure metacherts (Figure 5F, G). The BIFs show mm- to cm-thick bands of magnetite alternating with minor proportions of recrystallized quartz. Goethite and limonite may also be present.

Clastic rocks occur subordinated in centimetric lenses represented by very fine meta-arenites, carbonaceous phyllites and ferruginous metapelites (Figure 5H), commonly foliated. The metapelites are laminated, comprising fine-grained (chlorite)-biotite-quartz-mica schists and magnetite-quartz-chlorite schists. The carbonaceous phyllites are composed of quartz, sericite, chlorite, and carbonaceous matter. Metaconglomerates occur close to the tectonic contact between this unit and the Divinópolis Complex and the Onça do Pitangui Formation (Figure 2). They show stretched clasts embedded in a silt-sized matrix composed of quartz, sericite and oxidized material. The clasts have the same composition as the matrix, with higher proportions of sericite.

4.1.1.1.3 Córrego Santa Bárbara Member

The Córrego Santa Bárbara Member crops out as narrow NW-SE trending lenses and layers, with thickness commonly between 100 and 200 m, but reaching up to 800 m in the westernmost part of the Pitangui Synclinorium. The type section occurs along the Santa Bárbara stream, in the west of the synclinorium (quadrangle SE.23-Z-C-IV-1-SO; Di Salvio et al. 2019b). Representative occurrences can be found in the north of the city of Conceição do Pará and along the Pará river (quadrangle SE.23-Z-C-IV-1-SO; Di Salvio et al. 2019b). Additionally, good outcrops occur in road and railway cuts in the city of Pará de Minas (quadrangle SE.23-Z-C-IV-4-NO; Féboli et al. 2019).

This member comprises mainly clastic-chemical metasedimentary rocks represented by centimetric to metric intercalations of carbonaceous, ferruginous or sericitic phyllites, metagreywackes, metacherts, ferruginous metacherts, BIFs and felsic metavolcaniclastic rocks. Mafic metavolcanic rocks occur as minor components. Graphitic and ferruginous phyllites are predominantly recorded in the central region of the area, to the NW of Pará de Minas city (Figure 2). In the western region of the synclinorium, sericite-quartz schists, metagreywackes and metacherts predominate, and show relevant layers up to 150 m thick of felsic metaignimbrites interlayered with sericitic phyllites and mafic metavolcanic rocks.

The phyllites have very fine to silt grain size, and are laminated and show cm-thick banding. The carbonaceous type (Figure 6A) is dark gray in color, while the sericitic type has ochre, beige and purple colors; and the ferruginous type is orange and red.

The metagreywackes are lithic and/or feldspathic, being represented by sericite-quartz schists, biotite-quartz-plagioclase schists and chloritoid-quartz-chlorite schists (Figure 6B-C). The lithic metagreywackes show fragments of metachert, rounded quartz clasts and coarse-grained quartz crystals with corrosion gulfs (Figure 6D), suggesting a volcaniclastic origin. The oxidized chloritoid, when present, forms millimetric aggregates (Figure 6B, E). Layers with iron oxide are commonly interspersed in the metagreywackes.

The occurrences of metapyroclastic rocks are restricted to the western region of the Pitangui Synclinorium, and are mainly classified as felsic metaignimbrites (Figure 6F). They show bluish quartz porphyroclasts, commonly with corrosion gulfs preserved (Figure 6G), and lithic fragments (pumice) in a sericitic matrix, composed of quartz, muscovite, sericite and plagioclase. Fragments of pumice are rounded to angular, formed of quartz, plagioclase and fine sericite, with a twisted appearance, which sometimes preserve vesicular texture (Figure 6H), with circular cavities still discernible.

The Córrego Santa Bárbara Member has great metallogenetic importance, because it hosts rocks with gold mineralization of the Satinoco gold deposit (Figures 2 and 3), mainly at an amphibole-quartz shale level, and subordinately at a level composed of BIFs, with disseminated sulfide (Fabrício-Silva et al. 2021). The ore occurrence is related to a NW-SE shear zone, oblique to the stratification, which provided the percolation of hydrothermal fluids, allowing carbonation, silicification, sulfidation and gold input (Campos et al. 2008). Another mineral activity in this member is the extraction of carbonaceous phyllite at Fazenda Serra do Andaime, located approximately 10 km NW of Pará de Minas city.

4.1.1.2 Rio São João Formation

The Rio São João Formation is here proposed to assign the intermediate unit of the Pitangui Group (Figures 2 and 3), which mainly occurs as NW-SE- trending strips in the northeastern and southwestern limbs of the Pitangui Synclinorium. Its type area is located near the banks of São João River (quadrangle SE.23-Z.C-IV-1-SE; Brito et al. 2019b), and representative exposures also occur along the Alegria, Rio do Peixe and Grotão ridges, and at the north of the village of Jaguara, close to Ferreiras ridge (Figure 2). In the latter, this unit crops out in a W-E trending, and reaches 1000 m of thickness.

The contact with the underlying rocks of the Rio Pará Formation is transitional, being characterized by a gradual increase in siliciclastic lithologies and a decrease in mafic rocks. According to Brando-Soares et al. (2020), in this transition, the mafic rocks give place to calc-alkaline andesites. The contact

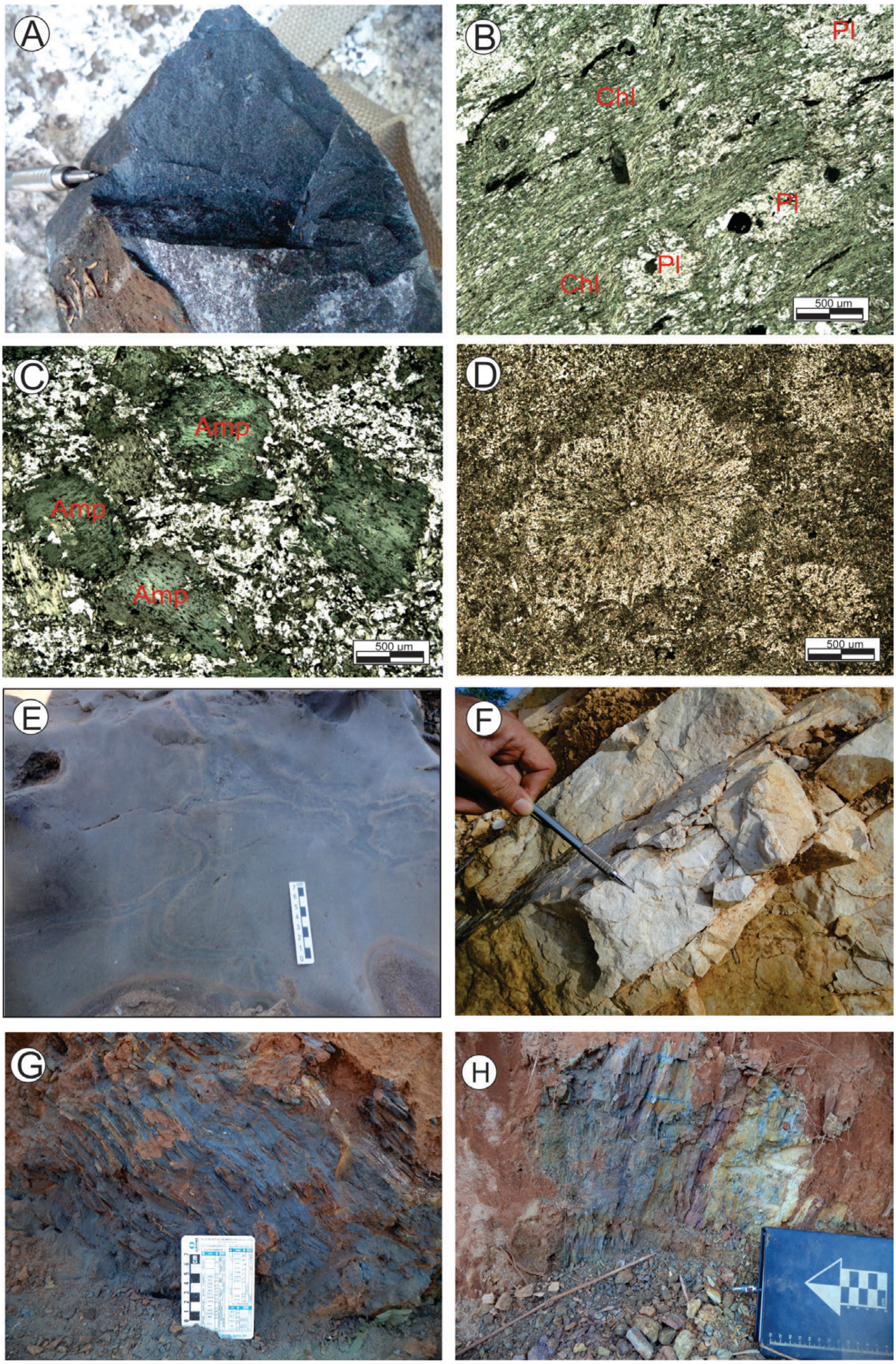

FIGURE 5. Velho do Taipa Member. A) Hand sample of a metabasalt with aphanitic texture; B) Photomicrography of plagioclase porphyroclasts in a groundmass composed of chlorite and minor amount of plagioclase (PPL); C) Photomicrography of medium-grained amphibole porphyroclasts in a fine, granoblastic groundmass with plagioclase and actinolite (PPL); D) Photomicrography of variolitic texture with plagioclase and amphibole needles forming fibro-radiated aggregates (PPL); E) Outcrop of pillowed metabasalt in the Pará River; F) Outcrop of decimetric metachert layer (ca. 40 cm thick) in mafic schist; G) Outcrop of banded iron formation; H) Outcrop of carbonaceous phyllite. Abbreviations: Chl = chlorite, Pl = plagioclase, Amp = amphibole.

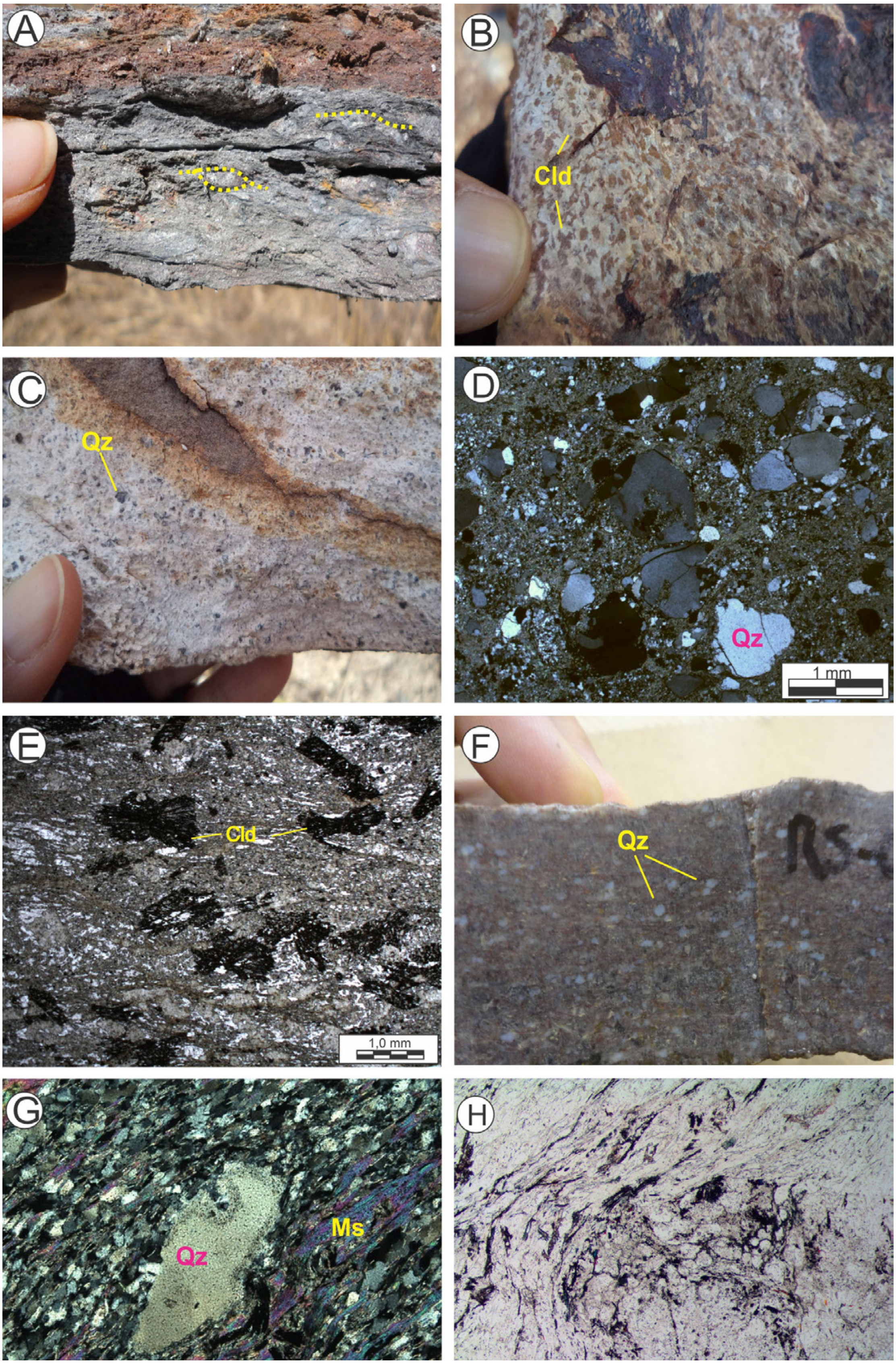

FIGURE 6. Córrego Santa Bárbara Member. A) Hand sample of carbonaceous phyllite showing mylonitic foliation (dashed lines); B) Hand sample of chloritoid-quartz-chlorite schist (metagreywacke) with oxidized chloritoid grains; C) Hand sample of lithic metagraywacke with coarse-grained smoky quartz crystals; D) Photomicrography of metagreywacke with coarse-grained quartz crystals with corrosion gulfs (CPL); E) Photomicrography of oxidized chloritoid grains in a chloritoid-quartz-chlorite schist (PPL); F) Hand sample of felsic metaignimbrite with bluish quartz porphyroclasts; G) Photomicrography of metaignimbrite with quartz clast showing corrosion feature (CPL); H) Photomicrography of pumice fragment (PPL). Abbreviations: Cld = chloritoid, Qz = quartz, Ms = muscovite.

with the Casquilho and Córrego do Arruda granites, and also with the Onça do Pitangui Formation, are marked by the NW-SE-oriented Pará de Minas transpressional shear zone (Figure 2), which imprinted a well-developed mylonitic foliation in the lithologies of this formation.

Previously, Romano and Carmo (1992) positioned the rocks of this unit at the base of the metavolcano-sedimentary sequence. Later, Romano (2007) defined it as a metasedimentary sequence, predominantly metapelitic with thin lenses of BIFs, carbonaceous phyllites and magnetitites. More recently, Brando-Soares et al. (2017) placed this formation at the base of the intermediate section of the greenstone.

Here, formally defined as Rio São João Formation, this unit is predominantly constituted of rhythmic metapelites, volcanogenic metagreywackes and metadiamictites, associated with metacherts and BIFs, in addition to restricted lenses of metamafic to metaultramafic rocks. These rocks can show intense carbonatation.

Metapelites exhibit rhythmic alternation of silt- to clay-rich layers, mm- to cm-thick, and are characterized by brown-orange to yellowish colors when weathered (Figure 7A). They also occur homogeneously or finely banded, with a predominance of clay-sized minerals. The rocks are generally well foliated and classified as quartz-biotite phyllite and quartz-chlorite-biotite phyllite. Under the microscope, they show a chloritic-biotitic matrix, involving quartz and feldspar grains and aggregates.

Volcanogenic metagreywackes show greenish-gray (Figure 7B) to light gray (Figure 7C) colors, and when weathered, reddish to yellowish shades. They commonly present a mm-scale compositional banding (Figure 7D) given by the variable amounts of quartz, chlorite, sericite and biotite. Quartz and plagioclase occur as porphyroclasts and commonly exhibit corrosion features. Lithoclasts are represented by fragments of metachert, metapelite and metamafic rocks.

Metadiamictite layers up to 200 m in width can be observed both on the southwestern (Sampaio 2019) and northeastern limbs of the Pitangui Synclinorium. These metadiamictites have clay to sandy-clay, greenish matrix (Figure 7E) composed of quartz, chlorite, amphibole, sericite, biotite, plagioclase, tourmaline, opaque and rare epidote and rutile. They show angular to rounded clasts up to 6 cm, represented by granules and/or pebbles of quartz, plagioclase, metachert (Figure 7F), metapelites, metamafic rocks, metaintermediate and metaultramafic rocks.

Intercalations of BIFs and metacherts in this sequence occur as decimetric layers (Figure 7G), up to 50 m thick. BIFs are fine-grained, laminated and formed of magnetite-rich levels alternating with quartz-rich bands (Figure 7H).

The mafic rocks are usually interlayered with the metapelitic sequence as thin cm- to dm-layers. They have fine to medium-grained texture, greenish colors and are composed of hornblende-actinolite, plagioclase, quartz, Fe-chlorite and biotite, characterized by plagioclase-actinolite schists.

Intercalations of BIFs and metacherts in this sequence occur as decimetric layers (Figure 7G), up to 50 m thick. These lithologies can also be seen intercalating talc schists. At the north of the village of Jaguara, they are associated with a hydrothermal alteration zone with carbonation and sulfidation, locally with massive magnetitites and tourmalinites. The BIFs are fine-grained, composed of quartz, magnetite (often martitized), hematite, goethite, sericite, chlorite and limonite pseudomorphs. They show laminated structure formed of magnetite-rich levels alternating with quartz-rich bands (Figure 7H). Centimetric layers of metalimestone, metachert and coarse-grained meta-arenite showing intense carbonatization, in addition to disseminated sulfides, also occur.

4.1.1.3 Onça do Pitangui Formation

The Onça do Pitangui Formation is the upper unit of the Pitangui Group and is here defined to enclose the clastic rocks located around the cities of Pitangui and Onça do Pitangui. These lithologies are formally subdivided into two members (Figures 2 and 3): Córrego Santo Antônio (pelitic-sandy metasedimentary) and Ribeirão da Onça (pelitic metasedimentary). Previously, Romano (2007) assigned these rocks to the top of a metavolcano-sedimentary and metasedimentary sequence. This formation occurs preferentially on the southwestern flank of the Pitangui Synclinorium and is expressed as a NW-SE elongated unit, following the Penha-Onça Lineament (Figure 2). There are good exposures in the vicinity of the cities of Onça do Pitangui and Pitangui. To the south, it is limited by the Rio São João Formation, and to the west and east, by the Rio Pará Formation. The contacts with both formations are tectonic, represented by faults and transpressional shear zones. The Onça do Pitangui rocks extend further to the northwest, where they are overlapped by Proterozoic metasedimentary rocks of the Fazenda Tapera Formation and Bambuí Group, besides the laterite cover.

4.1.1.3.1 Córrego Santo Antônio Member

The Córrego Santo Antônio Member crops out in the surroundings of the city of Onça do Pitangui (Figure 2; Quadrangles SE.23-Z-C-IV-1-SE, SE.23-Z-C-IV-3-NE, SE.23-Z-C-IV-2-SO, SE.23-Z-C-IV-4-NO, Brito et al. 2019b; Brito and Marinho 2019; Féboli and Marinho 2019b; Féboli et al. 2019) with thicknesses up to 1500 m. This unit overlaps the Rio São João Formation at the southwestern sector of the Pitangui Synclinorium, through transpressional tectonic contact. At the northeast, the contact with the Córrego Santa Bárbara Member (Rio Pará Formation) is marked by indiscriminate shear zones, and to the north, it shows inferred contact with strongly hydrothermally-altered rocks of the Serra dos Ferreiras Unit. The type-section occurs in road cuts connecting the city of Onça do Pitangui to Ferreiras ridge and in the vicinity of the Antimes ridge. In general, the outcrops are slightly to moderately weathered, and their best occurrences take place in the interfluves and streams, close to the city of Onça do Pitangui. (Figure 2).

This member mainly includes feldspathic to lithic metagreywackes, with subordinate lithic meta-arenites, metapelites, metacherts and BIFs. The lithic metagreywakes and meta-arenites are greenish-grey, which become reddish-brown to purple when weathered. They are muscovite-quartz-sericite schist, quartz-plagioclase-sericite schist, (chlorite)-carbonate-plagioclase-quartz-sericite schist and sericite-quartz schist, with quartz and plagioclase grains and rock fragments, mainly metachert and quartzite. Alteration processes, such as sericitization, saussuritization, argillization, and carbonation, may occur. These rocks are generally foliated and sometimes crenulated, with grains

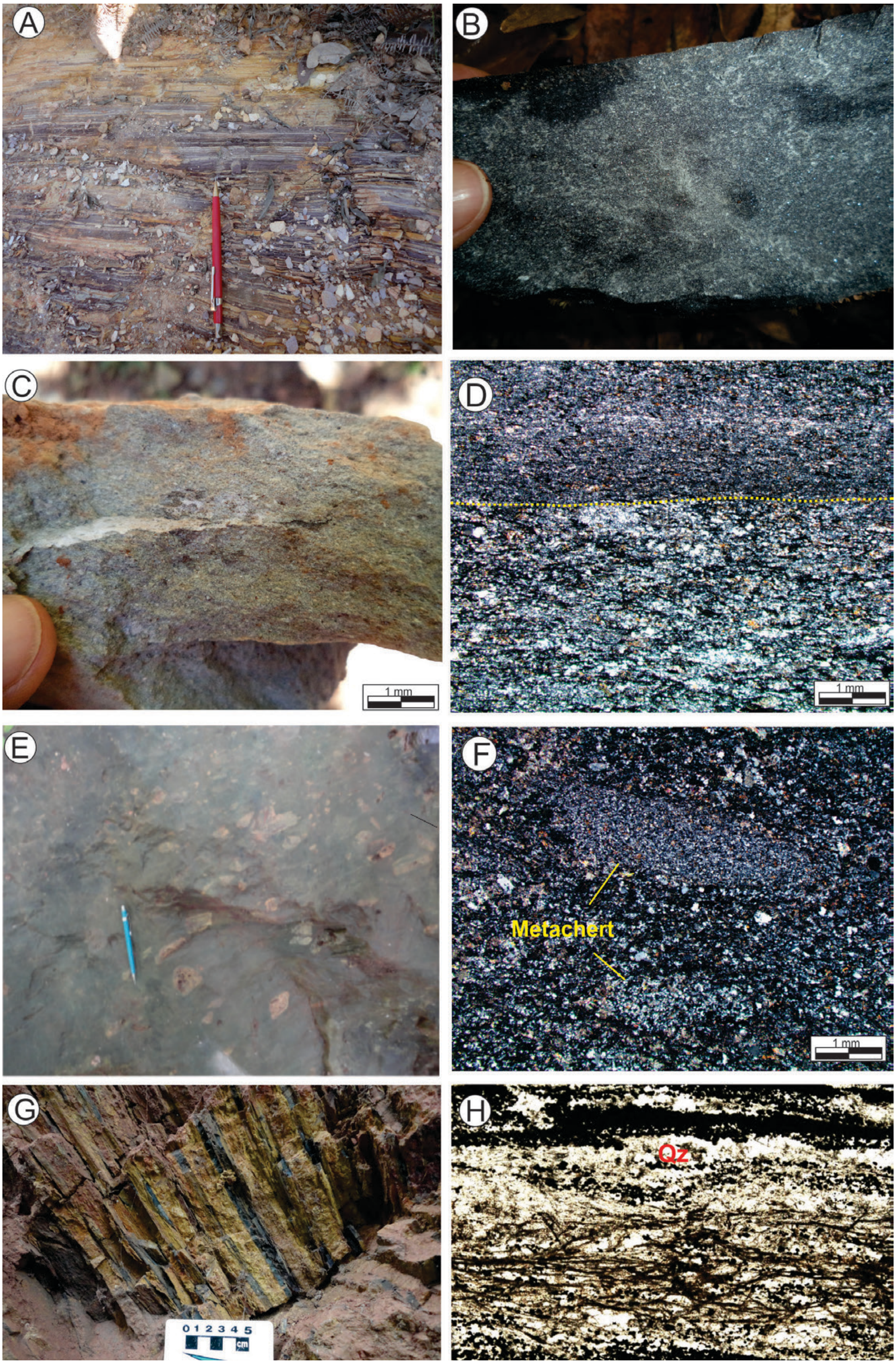

FIGURE 7. Rio São João Formation. A) Outcrop of rhythmic metapelite with alternation of silt- to clay-rich mm-thick layers; B) Hand sample of metagreywacke with greenish color; C) Hand sample of fine to coarse-grained metagreywacke; D) Photomicrography of a metagreywacke showing compositional banding highlighted by a yellow dashed line (CPL); E) Outcrop of polymictic metadiamictite with rounded to angular clasts of quartz, metachert, metapelite and mafic rock in a clay matrix; F) Photomicrography of metachert lithoclasts in a metadiamictite (CPL); G) Outcrop of cm-thick banded iron formation; H) Photomicrography of laminated compositional banding of a banded iron formation, characterized by magnetite and quartz-rich layers. Abbreviations: Qz = quartz, Mag = magnetite.

and lithoclasts stretched along the main foliation (Figure 8A). In the lithic meta-arenite, the coarser sand fractions predominate, while the metagreywacke has a predominance of fine fractions and is rich in a fine-grained matrix (Figure 8B) composed of quartz, plagioclase, sericite, biotite and chlorite. In metagreywackes, some quartz grains show possible corrosion features (Figure 8C), in a subhedral, prismatic shape, suggestive of volcanogenic origin. It may show mm- to cm-thick rhythmic lamination by alternating levels of varied sand granulometry (Figure 8D), and occasionally have microconglomeratic centimetric lenses (Figure 8E). Some samples also contain secondary carbonate as mineral aggregates or filling veins.

The metapelites are very fine- to fine-grained rocks, usually presenting rhythmic lamination (Figure 8F), and showing quartz grains in a foliated matrix, composed of sericite, chlorite, graphite and rutile. The contact with metagreywackes is sharp, highlighting the original bedding and the crenulated main foliation (Figure 8G). Subordinately, massive sericitic metapelites occur, made up of very fine sericite, involving porphyroclasts of oxidized mineral, subtly stretched along the foliation (Figure 8H).

Locally, carbonaceous phyllites are presented as millimetric to decimetric layers, being composed of sericite, quartz and carbonaceous matter. Layers of metachert and BIF occur locally near secondary shear zones, in the contact between this unit and the Rio Pará formation, in its northeastern portion (Figure 2). In this region, a NW-trending elongated body of BIF outcrops parallel to the Serra Grande shear zone.

4.1.1.3.2 Ribeirão da Onça Member

The Ribeirão da Onça Member comprises an elongated unit with NW-SE-trending, from the surroundings of the city of Pitangui to the Pará river margins (quadrangles SE.23-Z-C-IV-1-NO, SE.23-Z-C-IV-1-SO and SE.23-Z-C-IV-1-SE, Di Salvio et al. 2019a, 2019b; Brito et al. 2019b). It is estimated that this member has a thickness of up to 1200 m.

Metapelites are predominant in this member, presenting a pronounced plane-parallel rhythmic lamination of mm- to cm-thickness, with silty to silty-clay intercalations, showing normal grading cycles (Figure 9A). In general, these rocks have a quartz-sericite composition, sometimes with carbonaceous contribution, providing gray to purple colors (Figure 9B). They commonly present granules of quartz, oxidized material or kaolin (Figure 9C), and magnetite. These metapelites predominantly comprise quartz-sericite phyllite, sericite-quartz phyllite and chlorite-quartz phyllite that present an oblique foliation to the lamination (Figure 9D). At mylonitic levels, the foliation has an anastomosed aspect. Metaconglomerate layers occur at the base of this member. They show stretched clasts of metachert and ferruginous metachert immersed mainly in a fine sand-size matrix (Figure 9E).

The subordinated metagreywackes and meta-arkoses are schists with sub-rounded to sub-angular porphyroclasts of feldspar and quartz, in a fine-grained matrix containing variable proportions of quartz, sericite, and chlorite (Figure 9F). Carbonate is a late phase associated with fluid percolation. Feldspar grains are commonly sericitized and altered to clay minerals. These rocks are usually finely banded, showing levels with different granulometry, foliated to mylonitized, and sometimes show thin sheets of oxidized material and sericite. Intercalations of metacherts, laminated ferruginous metacherts (Figure 9G, H), BIFs and colorful phyllites also occur locally, at the base. Layers up to 100 m thick of BIFs and ferruginous metacherts stand out as crest elevation, possibly due to differential erosion. Metric to decametric smoky quartz veins, usually containing carbonate, are common in this unit. In the city of Pitangui (Figure 2), these veins are associated with the Penha-Onça lineament, and have metallogenic importance, since at the beginning of the 18th century there was an important artisanal gold mining in this locality.

4.1.2 Antimes Formation

The Antimes Formation is the upper stratigraphic unit of the greenstone belt sequence, and it was first defined by Romano (1989) to arrange the quartzitic rocks that cover the Pitangui Group. According to this author, it has a molassic origin and has a maximum thickness of 1000 m (Ritcher et al. 1975). This unit is composed of quartzites that were correlated to the Maquiné Group, which outcrops in the central portion of the Quadrilátero Ferrífero (Figure 1, Romano 1989, 2007; Romano and Carmo 1992). However, they were already considered to correspond to the rift-related rocks of the Minas Supergroup due to the occurrence of radioactive conglomerates (Richter et al. 1975; Frizzo et al. 1991; Teixeira and Kuyumjian 1991).

The Antimes Formation is best exposed in three areas. One NW-SE-trending layer in the northeast limb of the synclinorium, located west of the village of Pequi. The other two good exposures are located in the central region of the synclinorium, sustaining the Rio do Peixe, Alegria, Correias, Jaguara and Cruz do Monte ridges (Figure 2). Its type-area is located to the northeast of the city of Onça do Pitangui, in the Serra Grande ridge (quadrangle SE.23-Z-C-IV-1-SE, Brito et al. 2019b).

The contact with the Pitangui Group is characterized by an angular erosive unconformity. The contact with the Proterozoic metasedimentary rocks of Fazenda Tapera Formation and Bambui Group is tectonic by extensional faults.

The Antimes Formation is composed of pure to micaceous and/or ferruginous quartzites, associated with polymictic metaconglomerates at the base. Locally, intercalations of metapelites, hydrothermal rock layers and tectonic breccias occur. These breccias outcrop close to the basal contact of the unit and often present a magnetite-rich matrix. On the surface, levels of goethite, such as ferruginous crust, are common, as well as a ferruginous matrix in metaconglomerates.

Quartzites are light to dark gray when fresh (Figure 10A), and yellowish and friable when weathered. They are pure to micaceous, fine- to coarse-grained, with microconglomerate lenses (Figure 10B), which contain angular to rounded pebbles up to 2cm in diameter of smoky and milky quartz, metachert, sericitic phyllite, and, sometimes, grains of plagioclase and opaque minerals (possibly magnetite), in quartz-sericitic matrix (Figure 10C).

The petrographic analysis indicates pure quartzites with quartz grains with serrated boundaries and polygonal contacts (Figure 10D). Micaceous quartzites are predominantly sericitic, highlighting the prominent foliation (Figure 10E).

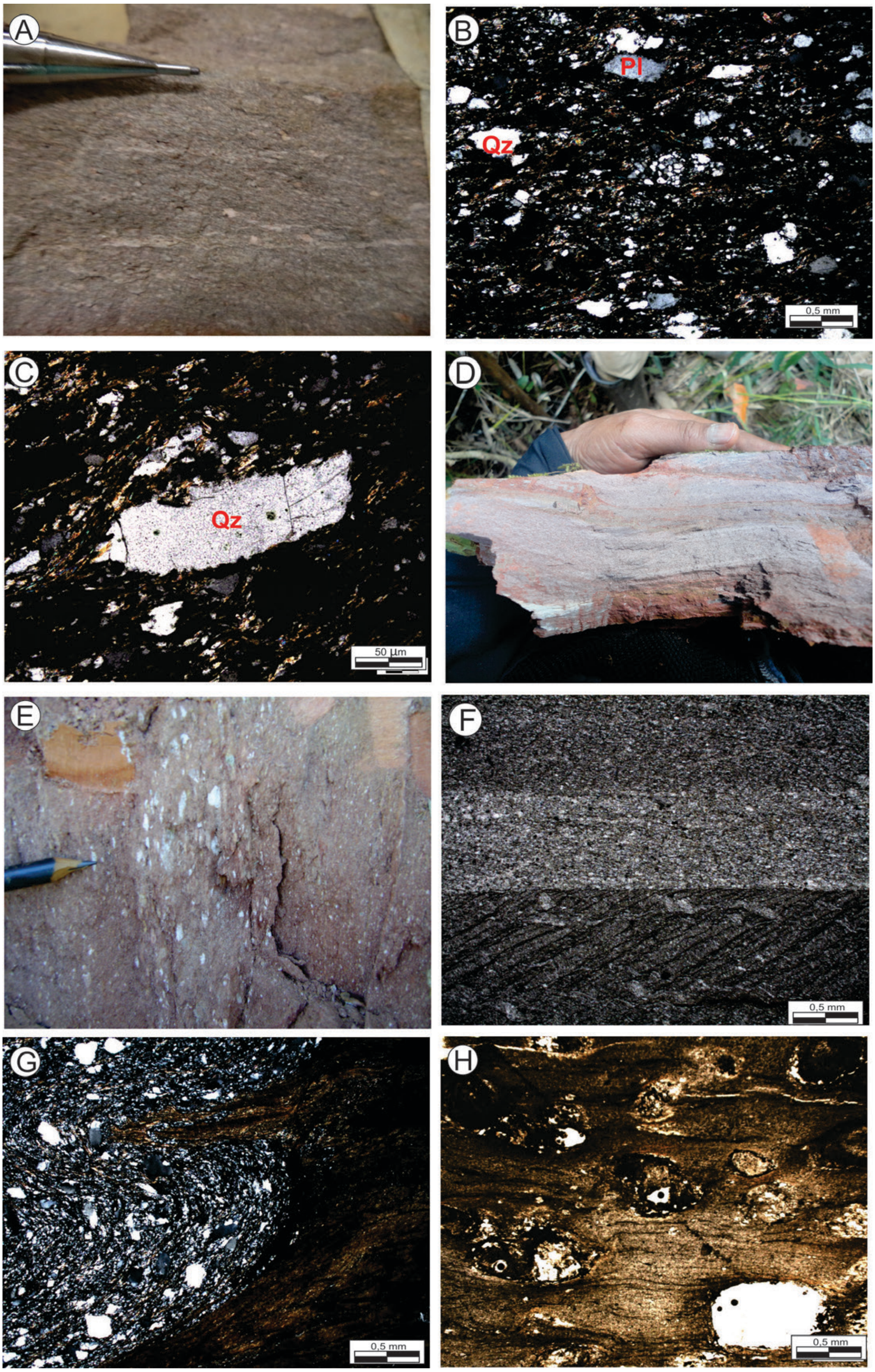

FIGURE 8. Córrego Santo Antônio Member. A) Hand sample of lithic metagreywacke with stretched granules and lithoclast along foliation; B) Photomicrography of metagreywacke showing quartz and plagioclase clasts (CPL); C) Photomicrography of prismatic quartz grain with possible corrosion features in a metagreywacke (CPL); D) Hand sample of laminated metagreywacke; E) Outcrop of metagreywacke with microconglomeratic levels composed of millimeter crystals of kaolinized feldspars and lithoclasts; F) Photomicrography of metapelite with rhythmic banding and well-developed crenulation cleavage in the finer-grained layer (CPL); G) Photomicrography showing the contact between metapelite and metagreywacke (bedding), and a crenulated foliation (CPL); H) Photomicrography of metapelite with porphyroclasts of oxidized mineral (CPL). Abbreviations: Qz = quartz, Pl = plagioclase.

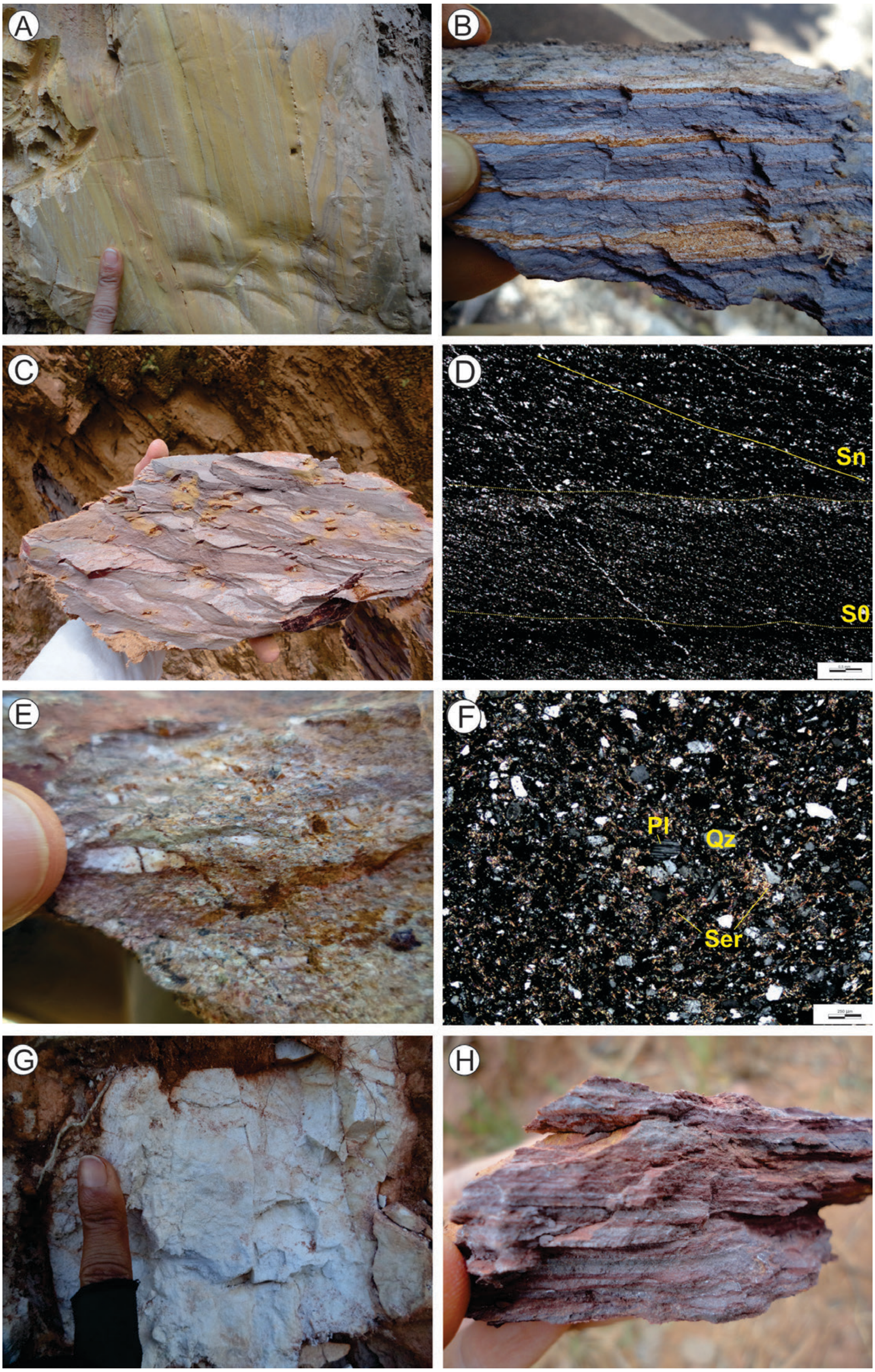

FIGURE 9. Ribeirão da Onça Member. A) Outcrop of metapelite showing millimeter to centimeter rhythmic banding; B) Hand sample of carbonaceous phyllite with millimeter to centimeter lamination; C) Hand sample of metarhythmite with granules of oxidized material, quartz and kaolin; D) Photomicrography of finely laminated quartz-sericitic metarhythmite showing foliation (Sn) oblique to bedding (S0; CPL); E) Hand sample of metaconglomerate with metachert clasts; F) Photomicrography of feldspathic metagreywacke exhibiting a very fine-grained sericitic matrix with porphyroclasts of feldspar and quartz (CPL); G) Hand sample of a whitish metachert; H) Hand sample of a BIF. Abbreviations: Qz = quartz, Pl = plagioclase, Ser = sericite.

Metaconglomerates show rounded to angular, gray to pinkish clasts of quartz, metacherts, phyllites and metamafic rocks, immersed in a dark gray, fine to medium-grained sandy matrix (Figure 10F). At Serra Grande ridge, drill hole surveys identified a basal polymictic conglomerate lens reaching up to 160 m thick, and containing pyrite, chalcopyrite and radioactive minerals (Ritcher et al. 1975). These authors describe mylonitic and cataclastic conglomerate lenses within the quartzite package, revealing samples with 0.05% of U_3O_8 and 2 g/t of gold. Close to the conglomeratic levels, pure quartzites with tabular (Figure 10G) and trough (Figure 10H) cross-beddings occur.

4.2 Serra dos Ferreiras Unit

The Serra dos Ferreiras Unit comprises hydrothermally altered rocks that occur as NW-SE metric lenses, reaching up to 2 km thick in places of greater exposure, as in its type-area at Ferreiras ridge, north of the city of Onça do Pitangui (Figures 2 and 3). These rocks have undefined stratigraphic positioning and may occur associated with different formations of the greenstone belt sequence, always associated with shear zones. In the region of the city of Pitangui, these rocks outcrop among the lithologies of the Onça do Pitangui Formation and are in irregular contact with the Antimes (upper) and Rio Pará (basal) formations. In the vicinity of Pará de Minas city, this unit occurs between the Rio Pará Formation and the Mato Dentro Suite, and also between the latter and the Córrego do Arruda Granite.

This unit is characterized by two types of hydrothermal alteration zones: sericite and peraluminous. The sericitic zones consist of schists with varying proportions of quartz, muscovite and chloritoid (Figure 11A), and may contain tourmaline, rutile (Figure 11B), kyanite and magnetite. They occur intercalated with muscovite quartzites, sometimes ferruginous. Restricted layers of sericitized metatuffs, metaconglomerates, carbonaceous phyllites, magnetitites and hematitites may occur.

The peraluminous alteration is associated to a peculiar rock known as agalmatolite, a schist containing pyrophyllite, quartz, diaspore, kyanite, muscovite and andalusite, which commonly shows pyrophyllite-rich spherical structures immersed in a thin phyllosilicate matrix (Figure 11C-E; Secco 2009). Luz et al. (2005) suggested that this rock is the product of hydrothermal alteration of several protoliths, including felsic and intermediate volcanic rocks and sedimentary rocks.

Different models for the genesis of this rock were proposed. Teixeira and Kuyumjian (1991) applied a hot spring model (post-volcanic hydrothermal alteration) with the Mato Dentro intrusive suite (Figure 2) as the source of the geothermal system. Carmo and Romano (1996) attribute that the regional tectonic evolution and a hydrothermal alteration by post-volcanic fluid were responsible for the origin of these rocks. On the other hand, Romano (2007) considers that this alteration process was developed by the dehydration of the sedimentary and volcanic-sedimentary pile of the Rio das Velhas Supergroup, during crustal shortening. However, post-magmatic fluids may also have contributed.

Agalmatolite has great economic importance in the region, which has more than 90% of the national resources of this mineral asset (DNPM 2010). The mining of agalmatolite began in the 1940s (Figure 11F) and has several industrial applications, such as paints, ceramics, thermal insulation, paper and cellulose treatment.

The subordinated felsic metatuffs present porphyroclasts of quartz and plagioclase with different shapes (angular, lenticular, acicular, pointed and corroded, occasionally showing embayments), and rare lithic particles (chert and pumice). The groundmass is composed of quartz, very fine sericite and rutile (Figure 11G, H). Zircon, chloritoid and tourmaline are accessory minerals. Although associated with sericite zones, these metatuffs occur close to the contact with the Onça do Pitangui Formation, and probably were originally correlated to this sequence.

4.3 Fazenda Tapera Formation

We propose in this study that the Fazenda Tapera Formation encloses the Rhyacian metasedimentary rocks (younger than 2132 ± 13 Ma; Brito et al. 2018) outcropping in the central and northwestern regions of the Pitangui Synclinorium, surrounding the locality of Rio do Peixe (Figure 2; Quadrangles SE.23-Z-C-IV-1-NE, SE.23-Z-C-IV-1-SE, SE.23-Z-C-IV-1-NO, SE.23-Z-C-IV-2-SO, Brito et al. 2019a, 2019b; Di Salvio et al. 2019a; Féboli and Marinho 2019b). This unit comprises an association of metagraywacke, metapelites and subordinate metatuffs, outcrops as a synform with NW-SE-trend and parallel axis, and was firstly characterized by this detailed mapping (Marinho et al. 2019).

These rocks were first described as metapelites and arkosic meta-arenites in the surroundings of the Rio do Peixe community, being correlated with the Proterozoic Minas Supergroup and Bambuí Group (Richter et al. 1975). Posteriorly, Romano (2007) associated the metasedimentary rocks in the northern region of the city of Pitangui with the Archean metavolcano-sedimentary sequence of the Nova Lima Group, Rio das Velhas Supergroup (Figure 2).

The Fazenda Tapera Formation overlaps the Archean lithologies of Onça do Pitangui and Antimes formations and is covered by the Neoproterozoic sedimentary rocks of the Bambuí Group by an erosive angular unconformity. Lateritic covers also occur over these units. This formation comprises two subunits named Engenho Velho and Fazenda Pacheco members (Figure 3).

4.3.1 Engenho Velho Member

The Engenho Velho Member mainly comprises silty-clay metarhythmites, with subordinate meta-arkose, lithic metagreywacke, metatuffs and metachert levels. This member is in transitional contact with the Fazenda Pacheco Member. Good outcrops occur in the central region of the Pitangui Synclinorium, to the southwest of Pequi (Figure 2). Other exposures are in the vicinity of the Rio do Peixe community and further west from there, in the vicinity of Barnabé and Bom Jardim streams.

The metarhythmites commonly show plane-parallel stratification (Figure 12A), and, locally, trough cross-bedding, wavy and lenticular structures (Figure 12B) (Cubas 2019). They are mainly composed of quartz, sericite and oxidized minerals, intercalating very fine to fine mm to cm bands. Meta-

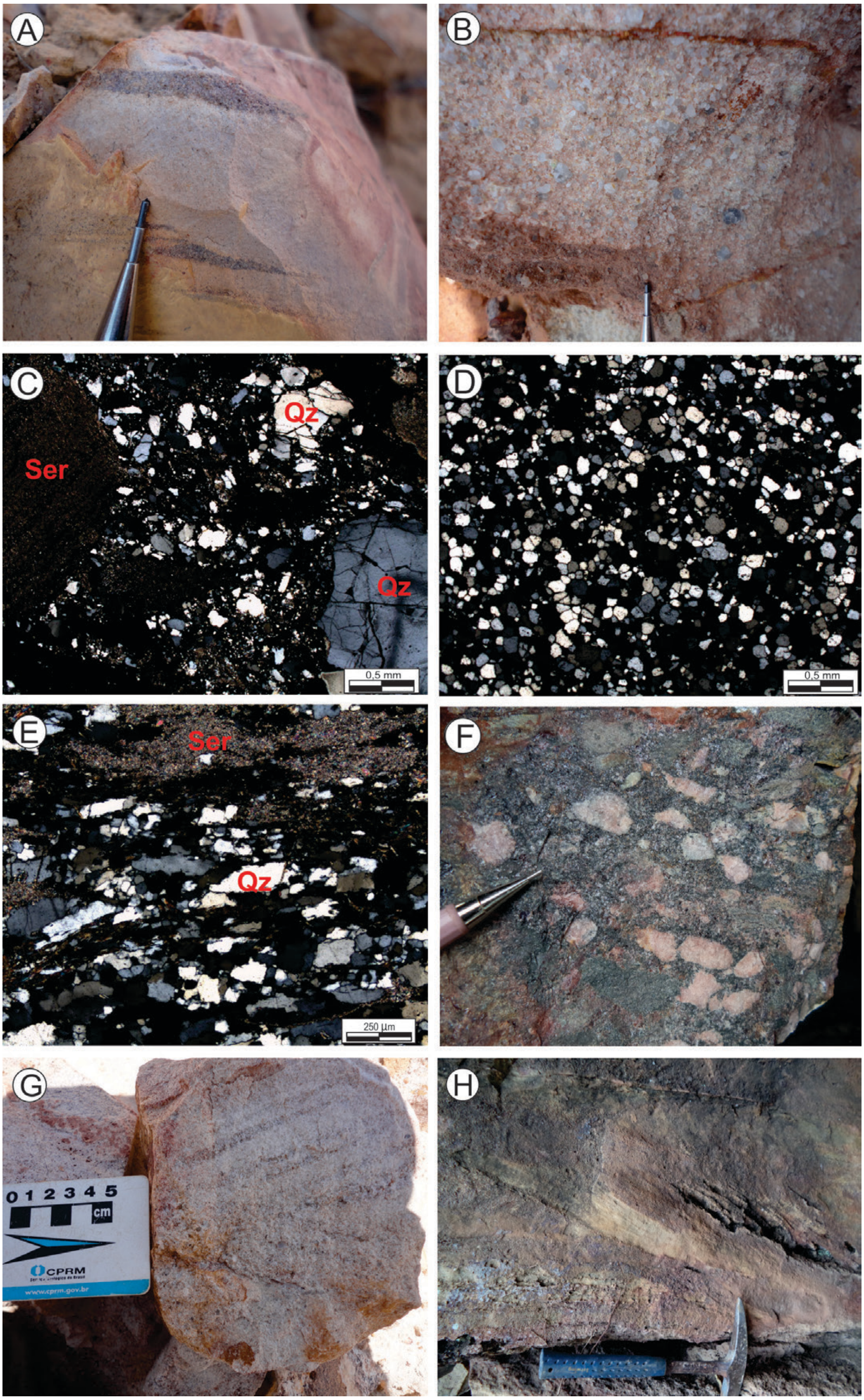

FIGURE 10. Antimes Formation. A) Hand sample of quartzite with centimetric banding; B) Hand sample of quartzite with microconglomerate lens composed of smoky and milky quartz granules and pebbles; C) Photomicrography of a microconglomerate layer in a quartzite (CPL); D) Photomicrography of impure quartzite with sericitic levels (CPL); E) Hand sample of polymictic metaconglomerate, with clasts of quartz and metapelite in a sandy matrix; F) Polymictic metaconglomerate with clasts of quartz, metachert and mafic rocks, in a sandy matrix; G) Outcrop of fine to coarse-grained quartzite with tabular cross bedding; H) Quartzite exhibiting medium-sized trough cross-bedding. Abbreviations: Qz = quartz, Ser = sericite.

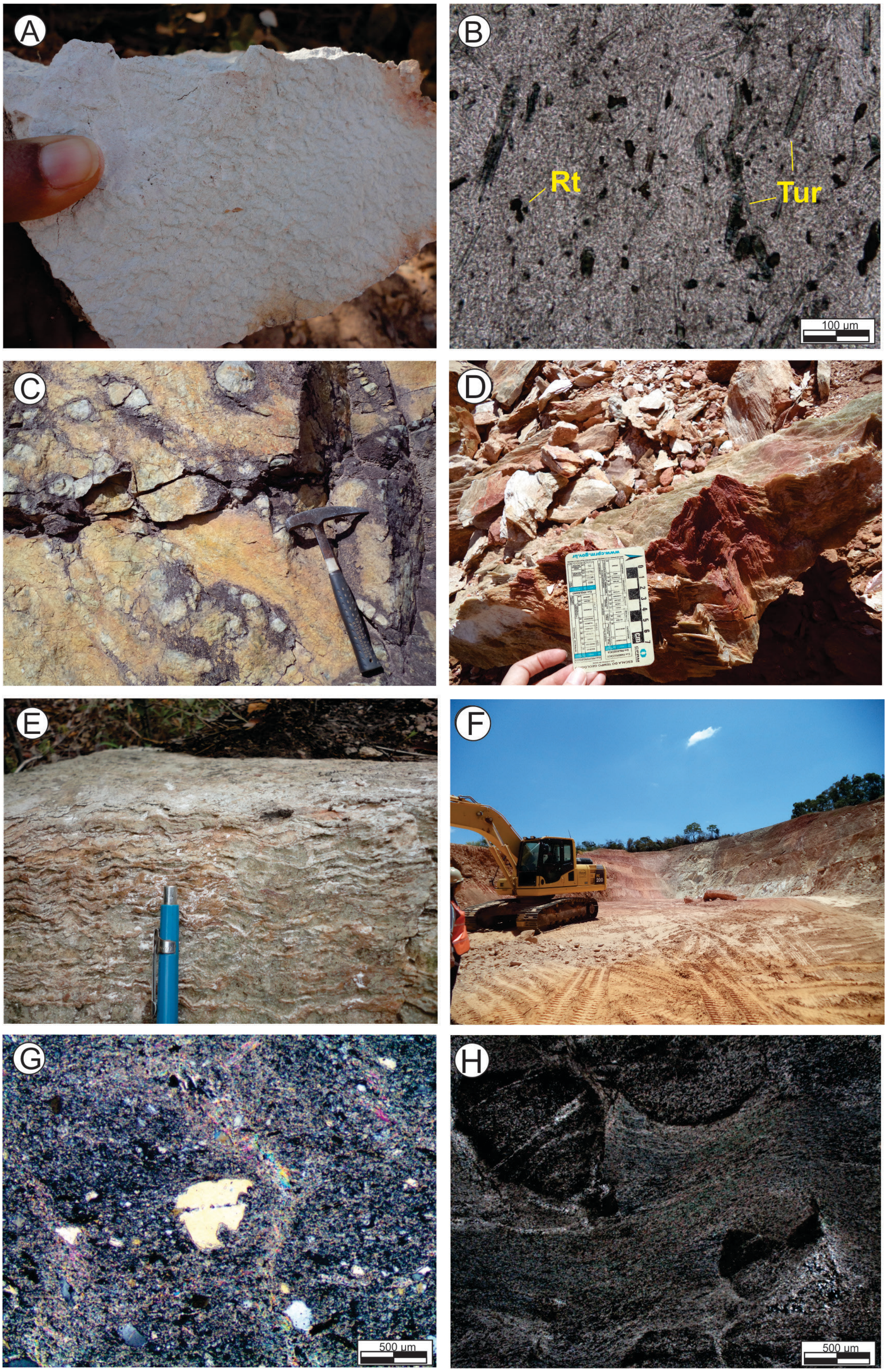

FIGURE 11. Serra dos Ferreiras Unit. A) Hand sample of schist in the sericitic alteration zone; B) Photomicrography of a muscovite schist from the sericitic zone, with prismatic crystals of tourmaline (Tur) and aggregates or isolated crystals of rutile (Rt; PPL); C) Outcrop of agalmatolite with green pyrophyllite-rich spherical structures; D), E) Samples of deformed agalmatolites, rich in pyrophyllite; F) Agalmatolite open pit mine of the Lamil Lage Minério Ltd; G) Photomicrography of fragmented felsic metatuff, composed of quartz with corrosion gulf and feldspar, in a phyllosilicate matrix (CPL); H) Photomicrography detailing the sericitic groundmass of the felsic metatuff (CPL).

arkose and lithic metagreywacke subordinately intercalate the pelitic sequence, in cm to m-thick layers. They are very fine to coarse sand-size, composed of quartz, plagioclase, sericite, chlorite, oxidized minerals and metachert fragments.

Metatuffs also occur interlayered in the sequence and can be divided in two types: with and without accretionary lapilli. The latter is white or gray clay lenses up to 30 cm thick, composed of a very fine sericitic groundmass, sharp and fine-grained quartz crystals and iron hydroxide particles of various shapes (needles, rods, angular or pointed fragments). Locally, these metatuffs present lozenge pseudomorphs of goethite up to 2 mm (Figure 12C, D). Felsic fallout metatuffs appear as metric to decimetric layers of a greenish-white, argillaceous rock, associated with metric metachert lenses. They are classified as sericite-quartz schists with rounded crystal fragments with goethite up to 3 mm. These fragments have a concentric zoned internal structure, with a quartz-sericite rim strongly impregnated with iron hydroxide and a clear core (Figure 12E, F), rich in microcrystalline to fine quartz, interpreted as accretionary lapilli. The groundmass is very fine-grained and composed of sericite, in which dispersed angular quartz grains (up to 0.2 mm) and weathered particles containing iron hydroxide with varied shapes (e.g. diamonds, rods, needles) occur. The presence of boxworks and disseminated euhedral crystals of pyrite in the metachert lenses suggest a possible hydrothermal alteration. An oblique foliation to bedding is recorded in these rocks.

4.3.2 Fazenda Pacheco Member

The Fazenda Pacheco Member crops out in the central area of the Pitangui Synclinorium, as a NW-SE layer at the south of Rio do Peixe locality, and a NE-SW layer at the northwest of this city (Figure 2). The best outcrops are located in road cuts near Fazenda Jaguara (SW of Pequi city) and on the banks of Cordeiro and Pintos streams, south of the city of Rio do Peixe. This unit is mainly composed of lithic meta-arenite, meta-arkose and metagreywacke, locally interbedded with centimetric to metric layers of laminated metapelites and lenses up to 50 centimeters of metatuffs. The internal structure of these rocks is massive to weakly foliated and, locally, shows trough and planar cross-bedding, besides small ripples (Cubas 2019). These metasandstones are very fine- to coarse-grained, with sand size up to 1.2 mm, predominantly angular and occasionally sub-rounded (Figure 13A, B). Inverse grading may be visible. They are composed of variable proportions of quartz, K-feldspar, plagioclase, opaque and lithic fragments. The lithoclasts range from 30 to 40%, are subangular to rounded, and are mainly represented by felsic volcanic rocks and chert, and subordinate clasts of granophyre and phyllite. The matrix varies from 10 to 20% and is very fine-grained, mainly formed by fine sericite and chlorite that tend to be oriented along the foliation plane, in addition to quartz and feldspar (Figure 13C, D). Biotite and very fine felsic argillaceous material may be present. Locally, intraclasts with a higher proportion of kaolin (Figure 13B) are observed.

The metapelites are mainly represented by metarhythmites with plane-parallel stratification, and composed of very fine to fine quartz, sericite and oxidized minerals in a silty-clay matrix. The thin lenses of metatuffs are composed of very fine sericitic groundmass, sharp quartz grains of fine sand to silt size and iron hydroxide particles. Locally, these metatuffs present goethite pseudomorphs up to 2 mm.

4.4 Mafic dikes and quartz veins

Among the several generations of mafic dikes mapped in the area, two of them have greater expression: one Paleoproterozoic and the other of unknown age. The former, attributed to the Pará de Minas dike system (Silva et al. 1995; Chaves and Neves 2005), is recognized mainly in the Onça do Pitangui Formation (Ribeirão da Onça Member), and generally occurs as rounded metric bodies, or sustaining small elongated ridges, with NW-SE trend (Figure 2). They are basic rocks, moderately weathered, composed of pyroxene, amphibole and chlorite. Phenocrysts of tabular to ripiform plagioclase were locally observed. Cederberg et al. (2016) assigned an age of 1702 ± 13 Ma (U-Pb in Badeleite) to a porphyritic gabbro in the south of Pitangui city.

The other dike system strikes at NE-SW and approximately N-S alignment, and intrudes the Mato Dentro Intrusive Suite, the Pará de Minas pluton, and the metarhythmites of Fazenda Tapera Formation (Engenho Velho Member). They are classified as gabbros and diabases.

Another feature highlighted in the region is the expressive rectilinear quartz veins, showing dozens of kilometers long and dozens of meters wide (Romano 2007). They are especially concentrated in the northeastern sector, with a NW-SE direction, in the rocks of the Maravilhas-Florestal Suite, in the Pequi Batholith.

4.5 Bambuí Group

The Neoproterozoic Bambuí Group, defined by Costa and Branco (1961) and later modified by Dardenne (1978, 1981), occurs in the central and northeastern sectors of the Pitangui Synclinorium, and also in the vicinity of the Pitangui and Onça do Pitangui cities (Figure 2). The deposition of this unit is controlled by normal faults. Its rocks cover the metasedimentary sequence of the Fazenda Tapera Formation by an angular erosive unconformity, and are in tectonic contact with the Antimes Formation, by extensional faults.

In the Pitangui Synclinorium, the Bambuí Group is represented by three formations, from base to top, Carrancas, Sete Lagoas and Serra de Santa Helena. Seismic data suggest that this unit reaches ca. 400 m depth, with its thickness increasing towards the north (Reis et al. 2017; Matos et al. 2022).

4.5.1 Carrancas Formation

The Carrancas Formation was first described by Costa and Branco (1961) as basal conglomerates. However, in the 1970s, Scholl (1976) interpreted this unit as a clastic facies of the Sete Lagoas Formation. More recently, Tuller et al. (2010) characterized two facies for the Carrancas Formation, from base to top: diamictite and rhythmite.

In the study area, it was divided in three members by Romano (2007): i) pelites and varvites related to a glacial sequence, ii) greywacke sandstones with lenses of diamictite with chloritic matrix, and iii) layers of arkosic to subarkosic sandstones.

To the northeast of the city of Onça do Pitangui, Romano and Knauer (2003) described dropped boulders in rhythmites of this formation. In the vicinity of the same city, three sections were characterized by Uhlein (2014): conglomerates at the base; greywacke sandstones, rhythmites and pelites at the intermediate section; and dolomites at the top.

In the scope of this study, the Carrancas Formation was subdivided into two members: (i) the Córrego Mata Vaca Member (base), represented predominantly by diamictites; and (ii) the Córrego Água Quente Member (top), characterized by claystones and rhythmites. The greywacke sandstones mapped by Uhlein (2014) were inserted here in the Fazenda Tapera Formation, while the dolomites were grouped in the Sete Lagoas Formation, as previously suggested by Romano (2007).

4.5.1.1 Córrego Mata Vaca Member

Diamictites related to the Córrego Mata Vaca Member outcrop as thin and restricted decametric lenses (quadrangles

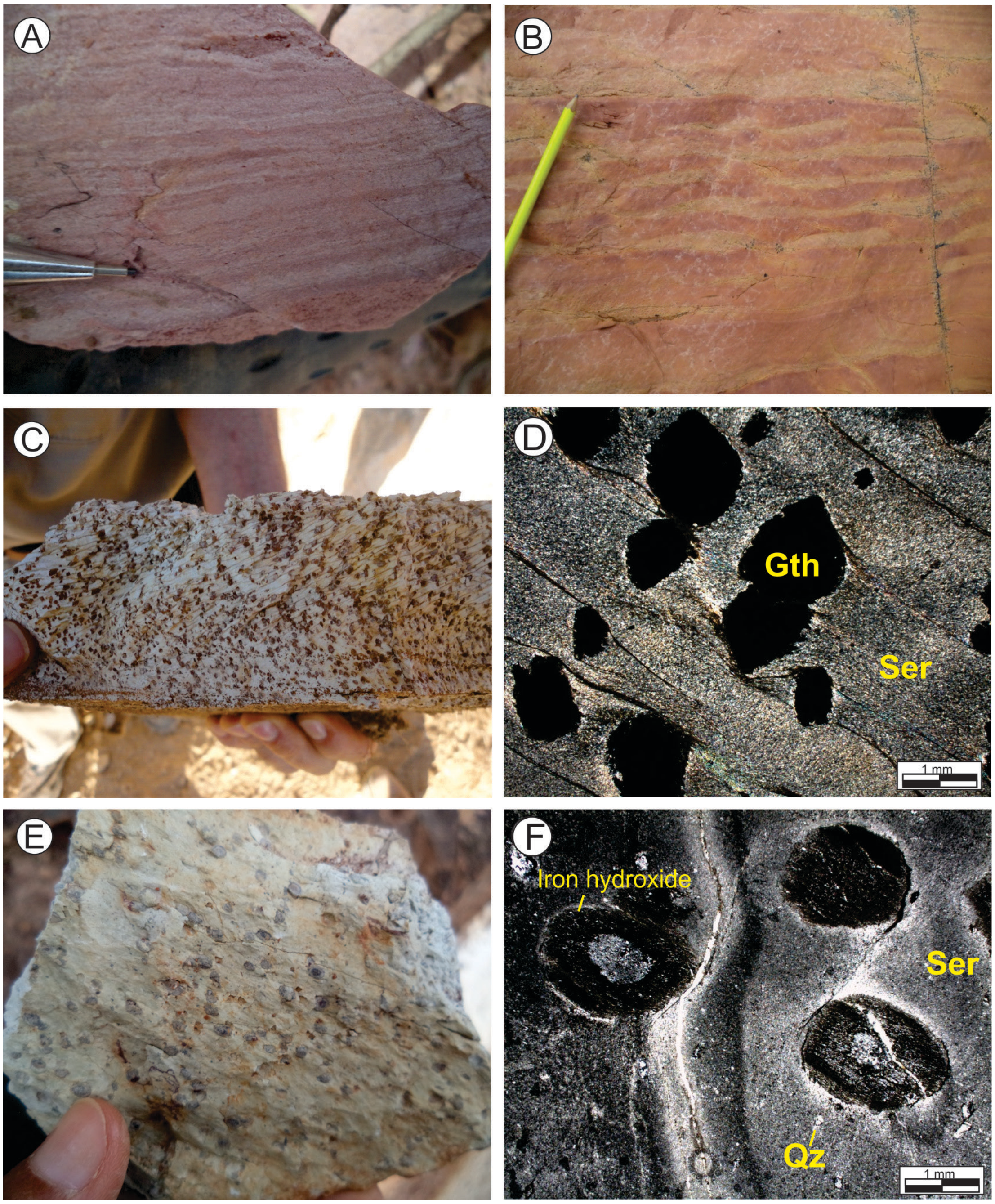

FIGURE 12. Engenho Velho Member. A) Hand sample of metarhythmite with pelitic-sandy lamination and plane-parallel stratification; B) Outcrop of metapelite showing wavy and lenticular structures; C) Hand sample of metatuff (sericite schist with disseminated goethite); D) Photomicrography of metatuff with goethite crystals (CPL); E) Hand sample of metatuff with accretionary lapilli represented by quartz-sericite phyllite; F) Photomicrography of metatuff (quartz-sericite phyllite) with concentric zoned fragments (accretionary lapilli) (CPL). Abbreviations: Gth = goethite, Ser = sericite, Qz = quartz.

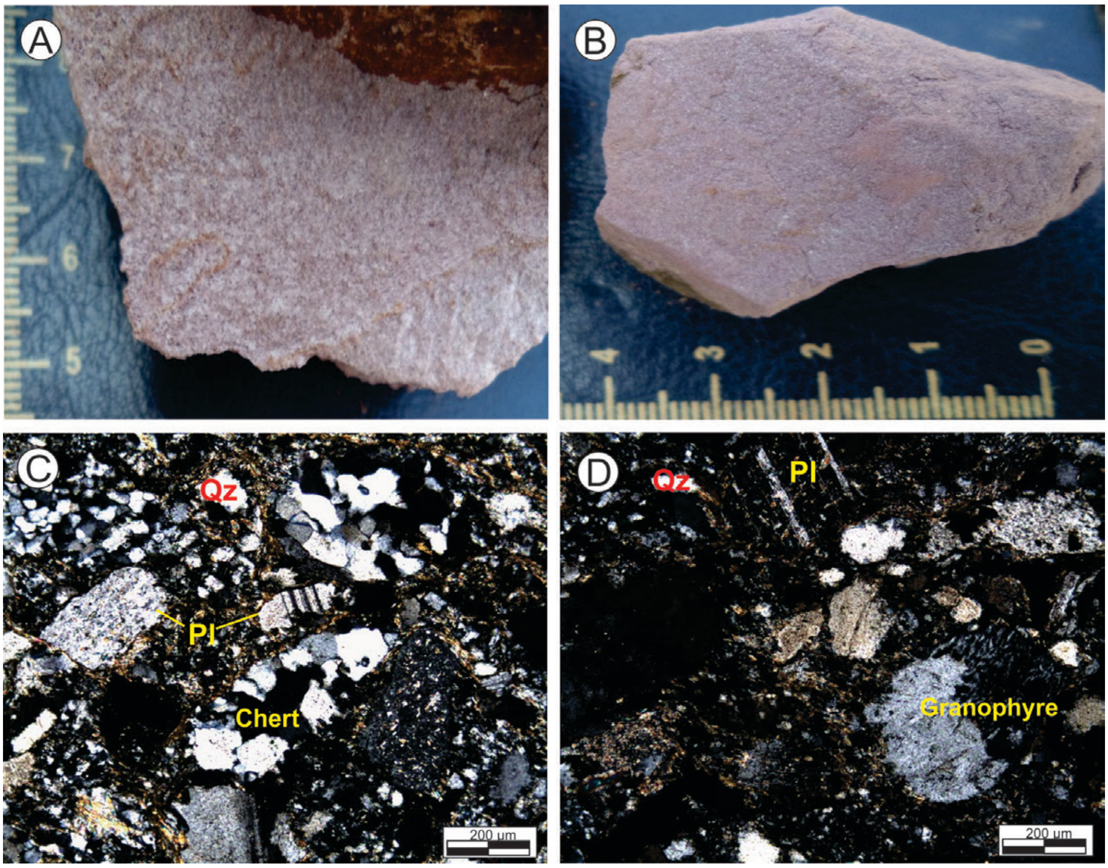

FIGURE 13. Fazenda Pacheco Member. A) Hand sample of coarse- (left) and fine-grained (right) metalithic arenite; B) Hand sample of fine to medium-grained meta-arkose with oriented kaolinitic intraclasts; C) Photomicrography of clast-supported lithic meta-arenite, with metachert, quartz and plagioclase (CPL); D) Photomicrography of metalithic-arenite showing fine-grained sericitic matrix. Abbreviations: Qz = quartz, Pl = plagioclase.

SE.23-Z-C-IV-1-NE, Brito et al. 2019a, and SE.23-Z-C-IV-2-SO, Féboli and Marinho 2019b). The best preserved outcrop occurs on the bed of the Peixe River (Figure 14A), and is constituted by rounded to angular clasts of granitoid, quartzite, silexite, limestone, quartz vein and gneiss, ranging from granules to boulders (Figure 14B, C), in a greenish gray silty matrix, which increases in proportion to the top of the unit. Under the microscope, the fine- to medium-grained matrix is predominantly composed of quartz, sericite, K-feldspar and plagioclase, with subordinate carbonate, epidote and muscovite.

4.5.1.2 Córrego Água Quente Member

The Córrego Água Quente Member is predominantly represented by rhythmites with carbonaceous and ferruginous layers and lenses, and it generally occurs in flatter reliefs. Its best exposure is in the SAFRAN quarry, in the northern foothills of Grande Rigde (quadrangle SE.23-Z-C-IV-2-SO, Féboli and Marinho 2019b), where a weathered sequence of fine and flat-parallel laminated pelites can be observed, showing mm to cm intercalations of silty to silty-sandy layers (Figure 14D). In this quarry, the rocks are smoothly folded (Figure 14E), with interstratal folding. Manganese concretions, with a botryoidal habit, also occur. Under the microscope, the pelite is characterized as a quartz-sericite phyllite with quartz grains immersed in a sericitic matrix (Figure 14F).

4.5.2 Sete Lagoas Formation

The Sete Lagoas Formation consists of dolomites, limestones and marly pelites (Dardenne 1978; Uhlein 2014), and it overlaps the diamictites of the Carrancas Formation. In the Pitangui Synclinorium, it occurs mainly in the central sector (Figure 2), surrounding the Ferreiras, Jaguara and Antimes ridges, where it has greater aerial exposure (quadrangle SE.23-Z-C-IV-1-SE, Brito et al. 2019b). Its best outcrops are located to the north of the city of Pitangui, along the banks of the Peixe River (quadrangle SE.23-Z-C-IV-1-NE, Brito et al. 2019a), and in an inactive quarry near the Campo Grande stream (quadrangle SE.23-Z-C-IV-1-NO, Di Salvio et al. 2019a).

In the study area, this unit is represented by: (i) laminated dolomites with decimetric layers of marl (Figure 15A); (ii) fine-grained calcarenites that locally show centimetric intraclasts (Figure 15B) and hummocky cross-stratification typical of tempestites (Figure 15C); (iii) laminated and ferruginous marls (Figure 15D) mainly composed of carbonates, with subordinate quartz, feldspar, sericite and oxides (Figure 15E-F).

4.5.3 Serra de Santa Helena Formation

The Serra de Santa Helena Formation is the unit of the Bambuí Group with the greatest aerial distribution, and it is composed of slates (Costa and Branco 1961), shales and siltstones with limestone lenses (Dardenne 1978).

In the studied area, this unit occurs at the south of the city of Rio do Peixe, bordering the Pará River in the extreme northwest of the mapped area, and also at the west of the city of Pitangui (Figure 2; quadrangles SE.23-Z-C-IV-1-NE, SE.23-Z-C-IV-1-SE, SE.23-Z-C-IV-1-NO and SE.23-Z-C-IV-1-SO, respectively, Brito et al. 2019a, 2019b; Di Salvio et al. 2019a, 2019b). The outcrops are generally weathered and preferably occur in road and highway cuts (Figure 16A). Its lithologies are represented by a succession of beige to gray rhythmites, showing fine plane-parallel stratification (Figure 16B), commonly with millimetric to centimetric silty-clay and fine sand layers. Locally, they present lenses of fine sandstones, carbonaceous siltstones (Figure 16C), laminated siltstones (Figure 16D) and limestones.

5. Discussion

5.1 Depositional models

Based mainly on field and petrographic criteria, this section discusses the depositional environments of the metavolcano-sedimentary and sedimentary sequences recorded in the Pitangui Synclinorium and presents schematic models for its rock associations (Figure 17).

5.1.1 Pitangui greenstone belt sequence

The Rio das Velhas Supergroup in the study area records a complete greenstone belt sequence, represented by ultramafic

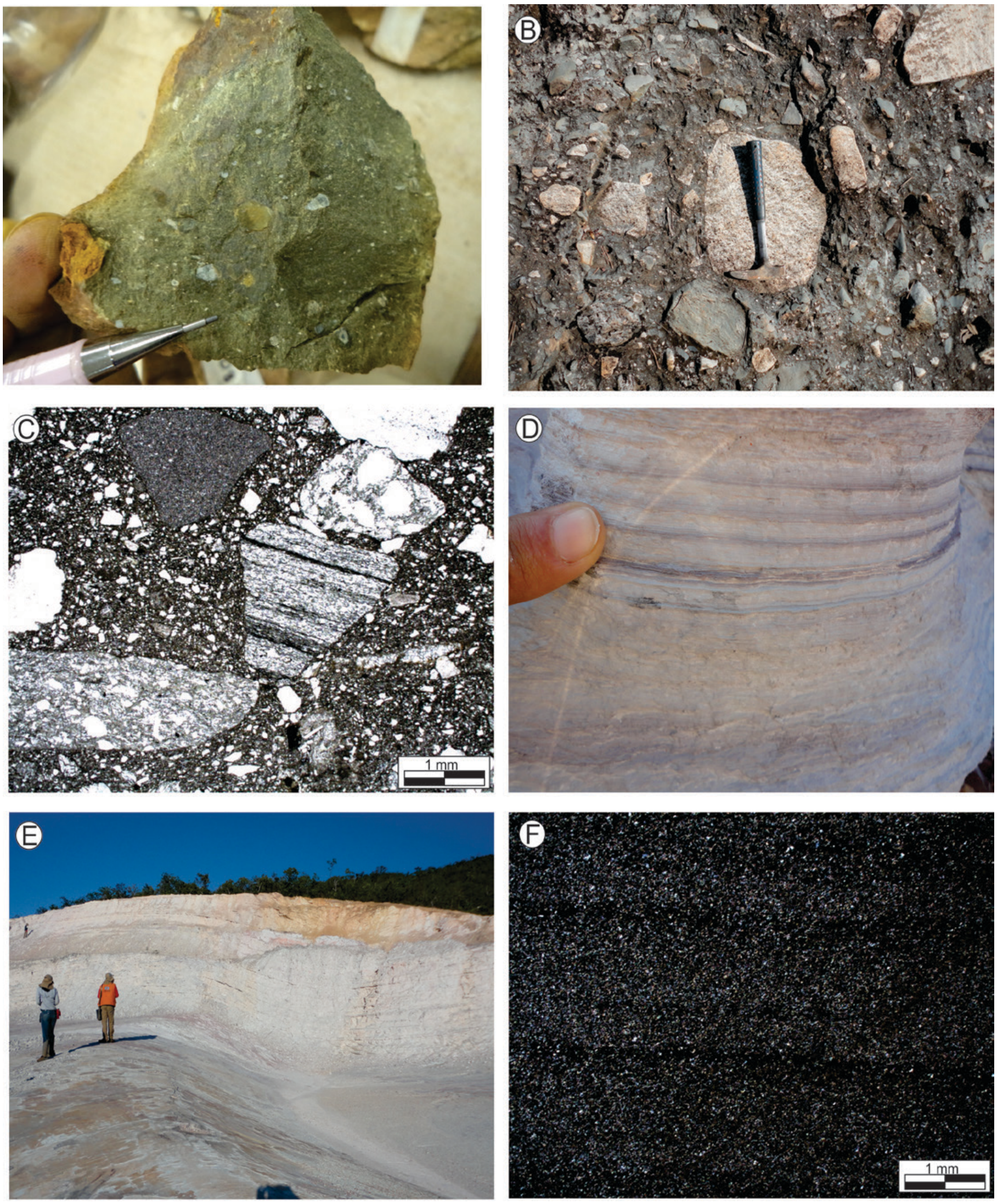

FIGURE 14. Carrancas Formation. A) Outcrop of diamictite (Mata Vaca Member) on the bed of the Peixe River; B) Detail of diamictite, with clasts of variable sizes of quartzites, granitoids and limestones; C) Photomicrography of the diamictite (PPL); D) laminated pelite of the Córrego Água Quente Member; E) Outcrop of a smoothly folded rhythmite; F) Photomicrography of a quartz-sericite phyllite (CPL).

FIGURE 15. Sete Lagoas Formation. A) Laminated dolomites; B) Hand sample of a calcarenite with intraclasts; C) Hummocky cross-stratification in calcarenite; D) Laminated and ferruginous marl; E) Photomicrography of a very fine-grained marl with a subtle bedding (PPL); F) Photomicrography of a marls showing a carbonate-rich matrix (CPL).

to felsic metavolcanic rocks, mafic to felsic metavolcaniclastic rocks and clastic-chemical metasedimentary rocks of the Pitangui Group, and clastic metasedimentary rocks of the Antimes Formation.

The basal formation of the greenstone belt sequence, represented by the Rio Pará Formation (Figure 3), is characterized by voluminous mafic volcanism closely associated with subordinated ultramafic magmatism (Figure 17A). The metaultramafic rocks are often strongly serpentinized and their primary mineralogy is completely replaced by hydrated phases. The presence of pillow-lava structures on metabasalts (Figure 5E) and chemical metasedimentary rock layers interbedded with the mafic-ultramafic rocks indicates a subaqueous environment for this rock association.

Furthermore, the restricted occurrence of felsic metaignimbrites and volcanogenic metagreywackes suggests the action of localized pyroclastic flows. Deposits of the former may have accumulated near steep volcanic cones, while the latter shows evidence of more intense reworking due to clast roundness, suggesting a distant volcanic source.

The intercalation of basic/ultrabasic and acid/intermediate magmatism (Figure 17A) implies a bimodal volcanic terrain. The chemical signature of the metabasalts of Rio Pará and Rio São João formations reveals a tholeiitic affinity and a trace element pattern similar to mid-ocean ridge basalts (Verma et al. 2017), while the intermediate rocks (mainly meta-andesites) show arc-affinity according to Melo-Silva et al. (2020) and Brando-Soares et al. (2020).

Metaignimbrite layers from the basal unit yielded a U-Pb zircon maximum depositional age at 2877 ± 4 Ma (Di Salvio et al. 2017), while Melo-Silva et al. (2020) obtained a 2740 ± 12 Ma crystallization age for a tholeiitic metabasalt, and a

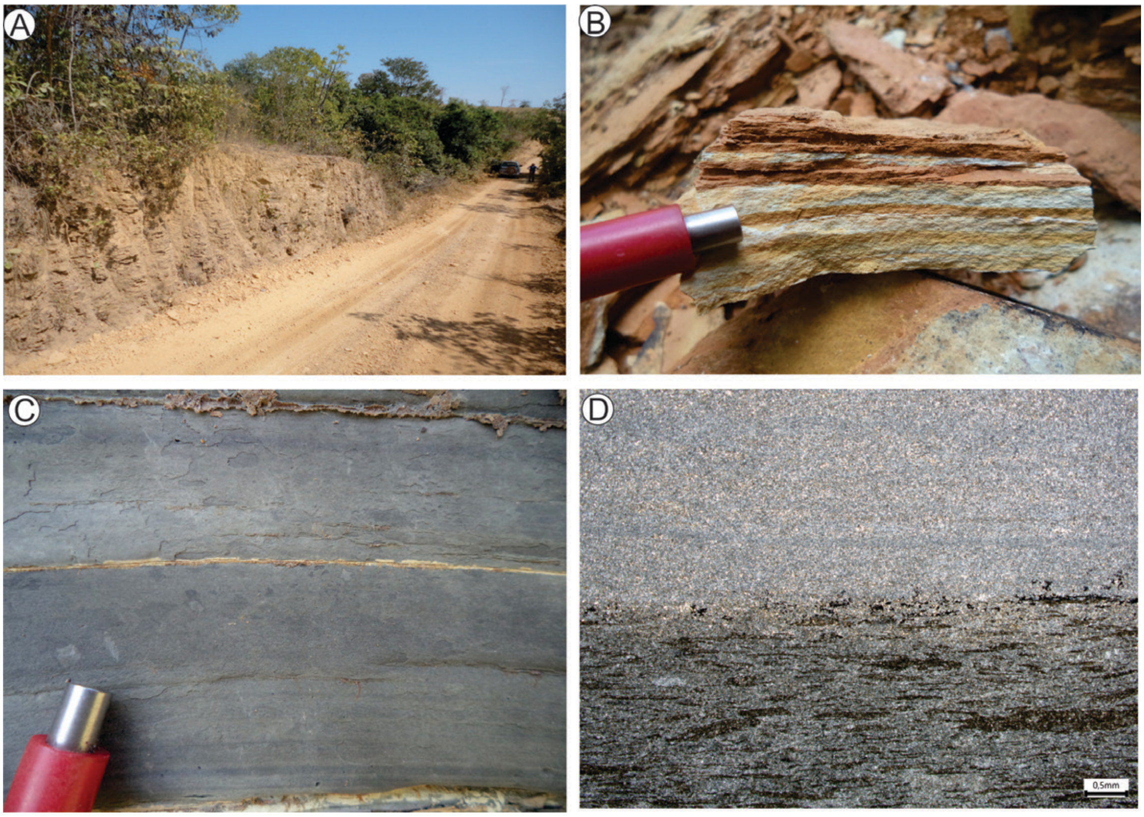

FIGURE 16. Santa Helena Formation. A) Aspects of the unit's highly weathered outcrops; B) Silty-clay rhythmite; C) Carbonaceous siltstone; D) Finely laminated siltstone.

maximum depositional age at 2770 ± 9 Ma for a metapelite. Additionally, Brando-Soares et al. (2017) present a U-Pb zircon maximum depositional age of 2859 ± 11 Ma for a meta-arenite.

The intermediate portion of the sequence includes the Rio São João and Onça do Pitangui formations, and presents a predominance of clastic-chemical sedimentation, represented by pelitic and sandy metasedimentary rocks, BIF and, subordinately, volcanogenic metagreywacke and metadiamictite (Figure 17A).

The clastic rocks were mainly formed by the reworking of the basal greenstone section, as suggested by the nature of their clasts and matrix compositions. It implies a hillier relief raised at this step of the basin evolution (Figure 17A) and the distribution of accommodation normal faults. The predominance of metapelites, metarhythmites and metagreywackes, and their close relation with chemical sediments, suggests deposition in a submarine fan system. The metadiamictites outcrop on both limbs of the synclinorium and could represent the proximal submarine fan system records. The association of clastic and chemical (mainly BIF) sedimentary rocks are formed by different styles of marine sedimentation. BIF deposition requires low-energy seawater (Beukes and Gutzmer 2008) that was periodically interrupted by influxes of clastic sediments from submarine fans. This alternation may have been caused by eustatic variations or by an interchange of tectonically active and inactive periods.

Volcanic activity, although present, has a secondary role. It is evidenced by the restricted lenses of mafic-ultramafic rocks, represented by metabasalts and metaserpentinites, denoting longer periods between the magmatic activity and a decrease in the eruptive products. A maximum depositional age of ca. 2.79 Ga was obtained by Marinho et al. (2017) from the metagreywackes of the intermediate portion.

The upper section of the greenstone belt sequence comprises metasedimentary rocks of the Antimes Formation, which overlies the Pitangui Group by an erosive discordance. This portion contains quartzites with preserved tabular and trough cross-bedding, and subordinated metaconglomerate lenses and metapelitic layers. Unlike the basal and intermediate sections, the field evidence suggests an essentially continental depositional environment for this unit, related to fluvial and fan delta systems, where the conglomerate lenses represent channel deposits (Figure 17B).

The stratigraphic position of this unit remains controversial. Previous correlations with Moeda Formation (Minas Supergroup; see section 4.1.2) take into account the occurrence of uraniferous conglomerates and the regional discordance with the greenstone belt sequence (Ritcher et al. 1975; Frizzo et al. 1991; Teixeira and Kuyumjian 1991).

Otherwise, recent U-Pb detrital zircon ages obtained in a metaconglomerate of this unit provided a maximum depositional age of ca. 2.69 Ga (Marinho et al. 2017), similar to the Maquiné Group (Moreira et al. 2016), which also contain U-occurrences.

The lower units of the greenstone belt, the exhumed TTG basement and Neoarchean granitoids sourced the sedimentation, which is characterized as a molasse sequence by Romano (1989, 2007). At that time, these older source rocks had already experienced the deformation of the Rio das Velhas II Orogenic Event (ca. 2.80 - 2.76 Ga; Farina et al. 2015, 2016). Thus, detailed stratigraphic and U-Pb detrital zircon provenance investigations are essential to define if

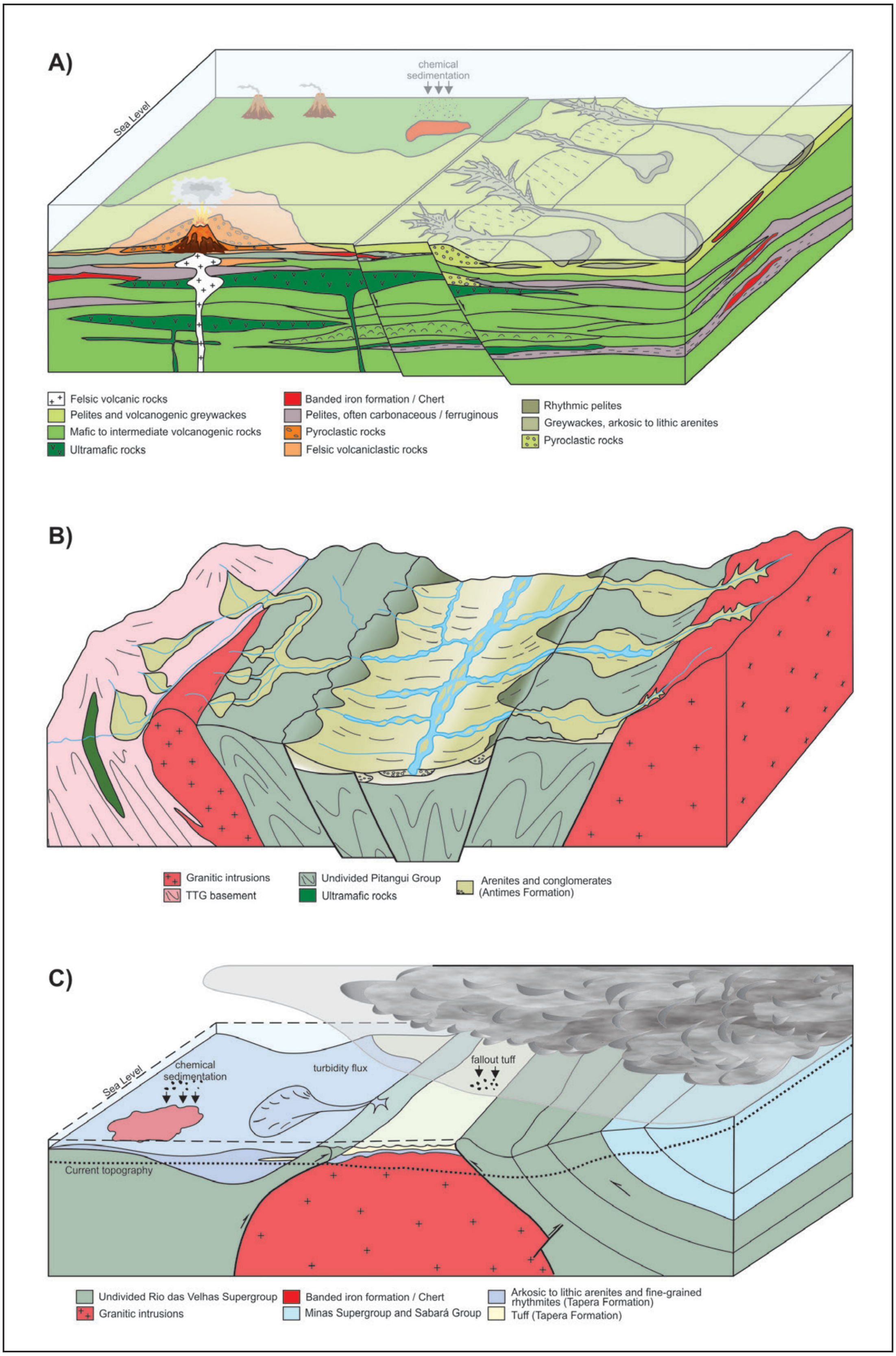

FIGURE 17. Depositional models for the Pitangui Synclinorium. (A) Pitangui Group: mafic/ultramafic basal volcanism with subordinated felsic rocks, transitioning to an intermediate succession dominated by clastic-chemical deposition. (B) Antimes Formation: essentially clastic sedimentation related to fluvial and fan delta systems. (C) Fazenda Tapera Formation: siliciclastic sequence deposited in a shallow marine environment, with subordinated chemical sedimentation and layers of tuff from distal volcanism.

this sequence belongs to the final stages of a Neoarchean orogeny or to the onset of the Minas basin.

5.1.2 Fazenda Tapera Formation

Newly described in this project, the Fazenda Tapera Formation is characterized by a siliciclastic package with alternation of expressive layers of fine (metapelites) and sandy materials (meta-arenites, metagreywackes and meta-arkoses), with subordinate layers of felsic metatuff and metachert. The sandy lithofacies show gradual coarsening upward, plane-parallel, cross and tabular bedding, and small ripples, in addition to wave and lenticular structures (Cubas 2019). This lithological succession, together with the internal structuring of the packages, corroborates the interpretation that the sediments were deposited in a shallow marine environment with variations in sea level. The sandy layers are associated with turbidity currents, while the pelitic facies represent the late stage of this current or a period of low energy between two turbiditic events. The deposition of metachert layers confirms the underwater environment.

The Engenho Velho Member is marked by the predominance of silty-clay metarhythmites over the sandy rocks, suggesting a prevalence of muddy, pelagic sedimentation, with eventual deposition of turbidite. Metric thicknesses of tuff and lapilli tuff layers interlayered with metachert suggest distal active volcanism with ash/fall deposits alternating with periods of quiescence and chemical deposition (Figure 17C).

In the Fazenda Pacheco Member, the predominance of sand-rich rocks in relation to the pelitic ones may reflect a shallowing-upward sedimentary cycle due to the coastal progradation (Tucker 2014). The presence of thinner tuff layers (maximum 50 cm thick) suggests a decrease in volcanic activity.

U-Pb zircon ages for meta-arenites yielded maximum depositional age of ca. 2132 ± 13 Ma (Brito et al. 2018). The younger source rocks for this unit are most likely associated with the Minas accretionary orogeny (ca. 2.5 - 2.1 Ga; e.g. Teixeira et al. 2015).

5.1.3 Bambuí Group

The upper sequence of the Pitangui Synclinorium is represented by the Carrancas, Sete Lagoas and Serra de Santa Helena formations, belonging to the Bambuí Group. This group has already been intensively studied by several authors, and in the region, the most recent works are from Uhlein (2014), Uhlein et al. (2012, 2016) and Reis et al. (2017).

Four second-order transgressive-regressive sequences were identified in the Bambuí Group by Reis et al. (2017). The Carrancas and Sete Lagoas formations are part of the first sequence, and the Serra de Santa Helena is included in the second one.

The Carrancas Formation is considered by some authors (Vieira et al. 2007, 2015; Romano 2007; Rocha-Campos et al. 2011; Kuchenbecker et al. 2013) as a continental unit of glaciogenic origin deposited on discontinuous channels of the basement in a low sea system tract, or deposited in grabens and semi-grabens during the interglacial interval (Uhlein et al. 2016). Romano and Knauer (2003) described dropped boulders in rhythmites of Córrego Água Quente Member, also suggesting a glaciogenic environment. Though possible, no direct glacial influence has been identified during our field surveys. Based on our observations, we suggest that the depositional environments of the Carrancas Formation corresponded to lacustrine or restricted marine settings subjected to turbidity currents depositing poorly sorted conglomerates (e.g., Eyles and Eyles 2000), as first proposed by Uhlein et al. (2012).

This formation is covered by dolomites, limestones, marly and carbonate-rich pelites from the Sete Lagoas Formation. In its type area, Vieira et al. (2007) individualized two retrogradational-progradational cycles for these carbonate ramp sediments, which record the interaction between rates of subsidence, eustatic oscillation and carbonate deposition. In the Pitangui Synclinorium, one retrogradational cycle is well preserved in an inactive quarry, in the west of Rio do Peixe locality. Calcarenite with hummocky cross-stratification, typical of shallow marine environment sedimentation, is overlapped by a package of about 40 m of limestone with plane parallel lamination. The former was deposited below the storm weather wave base. Thus, this sequence marks a sea level rise.

In the Pitangui Synclinorium, the Serra de Santa Helena formation is recorded by rhythmites, with subordinate fine sandstone, carbonaceous siltstone and limestone lenses. According to Reis et al. (2017), this formation is considered a transgressive-regressive system tract, from a carbonate ramp to a fine-grained predominantly siliciclastic succession of deep water, forming a maximum flooding surface. This surface is covered by a thick regressive succession that includes intercalations of sand and clay from deep water turbidites that grade to siliciclastic deposits of prodelta and delta front (Reis et al. 2017).

6. Conclusions

The stratigraphic sequence presented in this work for the Pitangui Synclinorium includes an Archean metavolcano-sedimentary sequence, belonging to the Pitangui Group and Antimes Formation; Paleoproterozoic clastic metasedimentary rocks of the Fazenda Tapera Formation; and a Neoproterozoic clastic-chemical sedimentary association of the Bambuí Group.

This contribution also reveals that the Archean greenstone belt sequence comprises metaultramafic rocks and tholeiitic metabasalts with felsic/intermediate metavolcanic and metavolcaniclastic rocks of the Rio Pará Formation, followed by a clastic-chemical metasedimentary succession with metavolcaniclastic rocks of the Rio São João Formation, and a clastic metasedimentary sequence of the Onça do Pitangui Formation, all belonging to the Pitangui Group. The upper siliciclastic metasedimentary rocks of the Antimes Formation complete the greenstone belt stratigraphy.

The voluminous basal mafic-ultramafic volcanism and subordinated pyroclastic rocks of the greenstone belt sequence erupted in a subaqueous environment, with minor chemical sedimentation associated. The following amount of metasedimentary rocks, which increased towards the top of the stratigraphic section, indicates the reworking of the basal units in a submarine fan system. Clastic sediments of the greenstone's upper formation are related to fluvial and fan delta systems in a continental environment.

The Paleoproterozoic Fazenda Tapera Formation mainly contains metarhythmites and arkosic meta-arenites, with local fallout metatuff and metachert layers. These rock associations were deposited in a shallow marine setting dependent upon sea level changes, with the action of turbidity currents and low energy periods, and also the influence of distal acid volcanism, which decreased towards the top of the unit.

The Neoproterozoic Bambuí Group includes diamictites, claystones and rhythmites of the Carrancas Formation; dolomites, calcarenites and marls of the Sete Lagoas Formation; and rhythmites with lenses of sandstone, siltstone and limestone of the Serra de Santa Helena Formation. The basal sedimentation of this group mainly records the activity of turbidity currents in a lacustrine or restricted marine environment. It is followed by significant clastic-chemical sediments deposited in shallow to deep marine waters, strongly controlled by transgressive-regressive phases.

Acknowledgments

We acknowledge the support provided by the Geological Survey of Brazil-CPRM. We are grateful to Fernanda Moura, Maria Oliveira and Anna Dreher for the support on the petrographic descriptions, to Elizabeth Costa by digitizing the depositional model, and to Ana Pires and Luiza Clemente for help in formatting the manuscript. The authors would also like to thank Camille Rossignol and two anonymous reviewers for constructive reviews that helped to improve the manuscript, as well as the Editor Evandro Klein.

Authorship credits

Author	A	B	C	D	E	F
MSM	■	■	■	■	■	■
JRM			■	■	■	
JCL	■	■	■	■	■	
JCSA			■	■	■	
LPPDS		■	■	■		
RNS		■	■	■		
DCB		■	■	■		
WLF		■	■			
CFB			■		■	

A - Study design/Conceptualization **B** - Investigation/Data acquisition
C - Data Interpretation/ Validation **D** - Writing
E - Review/Editing **F** - Supervision/Project administration

References

Alkmim F.F., Marshak S. 1998. Transamazonian Orogeny in the Southern São Francisco Craton Region, Minas Gerais, Brazil: evidence for Paleoproterozoic collision and collapse in the Quadrilátero Ferrífero. Precambrian Research, 90(1-2), 29–58. https://doi.org/10.1016/S0301-9268(98)00032-1

Araújo J.C.S., Ferreira R.C.F., Freitas F.M, Magalhães J.R. 2020. The Archean Rio das Velhas greenstone belt revisited: new insights into the stratigraphy. Journal of the Geological Survey of Brazil, 3(3), 113–149. https://doi.org/10.29396/jgsb.2020.v3.n3.1

Beukes N.J., Gutzmer J. 2008. Origin and paleoenvironmental significance of major iron formations at the archean-paleoproterozoic boundary. Reviews in Economic Geology, 15, 5–47. https://doi.org/10.5382/Rev.15.01

Brando-Soares M., Corrêa Neto A.V., Zeh A., Cabral A.R., Pereira L.F., Prado M.G.B., Almeida A.M., Manduca L.G., Silva P.H.M., Mabub R.O.A., Schlichta T.M. 2017. Geology of the Pitangui greenstone belt, Minas Gerais, Brazil: Stratigraphy, geochronology and BIF geochemistry. Precambrian Research, 291, 17-41. https://doi.org/10.1016/j.precamres.2017.01.008

Brando-Soares M., Corrêa Neto A.V., Bertolino L.C., Alves F.E.A., Almeida A.M., Silva P.H.M., Mabub R.O.A., Manduca L.G., Araújo I.M.C.P. 2018. Multistage mineralization at the hypozonal São Sebastião gold deposit, Pitangui greenstone belt, Minas Gerais, Brazil. Ore Geology Reviews, 102, 618–638. https://doi.org/10.1016/j.oregeorev.2018.09.028

Brando-Soares M., Corrêa Neto A.V., Fabricio-Silva W. 2020. The development of a Meso- to Neoarchean rifting-convergence-collision-collapse cycle over ancient thickened protocontinent in the South São Francisco Cráton, Brazil. Gondwana Research, 77, 40-66. https://doi.org/10.1016/j.precamres.2017.01.008

Brito D.C., Féboli W.L., Marinho M.S., Silva R.N., Di Salvio L.P.P., Dreher A.M., Silva M.A., Lombello J.C. 2018. Registro paleoproterozoico no sinclinório de Pitangui, noroeste do Quadrilátero Ferrífero, Minas Gerais, Brasil. In: Congresso Brasileiro de Geologia, 49, ST11, 7894. Available online at: http://www.sbgeo.org.br/home/pages/44 / (accessed on 10 March 2023).

Brito D.C., Marinho M.S., Lombello J.C. 2019a. Mapa geológico e de recursos minerais - Folha SE.23-Z-C-IV-1-NE, Escala 1:25.000. Projeto ARIM, Belo Horizonte, CPRM. Available online at: https://rigeo.cprm.gov.br/handle/doc/19406 / (accessed on 24 January 2023).

Brito D.C., Marinho M.S., Lombello J.C. 2019b. Mapa geológico e de recursos minerais - Folha SE.23-Z-C-IV-1-SE, Escala 1:25.000. Projeto ARIM, Belo Horizonte, CPRM. Available online at: https://rigeo.cprm.gov.br/handle/doc/19324 / (accessed on 24 January 2023).

Brito D.C., Marinho M.S. 2019c. Mapa geológico e de recursos minerais - Folha SE.23-Z-C-IV-3-NE, Escala 1:25.000. Projeto ARIM, Belo Horizonte, CPRM. Available online at: https://rigeo.cprm.gov.br/handle/doc/19167 / (accessed on 24 January 2023).

Campos W.F., Duchini Jr. J., Frizzo C. 2008. Projeto Ouro Turmalina, Alvo Satinoco, Quadrilátero Ferrífero/MG. Ouro Preto, Jaguar Mining Group, Simexmin.

Carmo J.C.C., Romano A.W. 1996. O agalmatolito de Minas Gerais e sua utilização como rocha industrial. Revista da Escola de Minas, 49(4), 39-44.

Carneiro M.A. 1992. O Complexo Metamórfico Bonfim Setentrional (Quadrilátero Ferrífero, Minas Gerais): Litoestratigrafia e evolução geológica de um segmento de crosta continental do Arqueano. PhD Thesis, Instituto de Geociências, Universidade de São Paulo, São Paulo, 233p. https://doi.org/10.11606/T.44.1992.tde-18112015-104751

Caxito F., Lana C., Frei R., Uhlein G.J., Sial A.N., Dantas E.L., Pinto A.G., Campos F.C., Galvão P., Warren L., Okubo J., Ganade C.E. 2021. Goldilocks at the dawn of complex life: mountains might have damaged Ediacaran–Cambrian ecosystems and prompted an early Cambrian greenhouse world. Scientific Reports, 11(1), 20010. https://doi.org/10.1038/s41598-021-99526-z

Cederberg J., Söderlund U., Oliveira E.P., Ernst R.E., Pisarevky S.A. 2016. U-Pb baddeleyite dating of the Proterozoic Pará de Minas dyke swarm in the São Francisco craton (Brazil) - implications for tectonic correlation with the Siberia, Congo and North China cratons. GFF, 138(1), 219−240. https://doi.org/10.1080/11035897.2015.1093543

Chaves A.O., Neves J.M.C. 2005. Magmatism, rifting and sedimentation related to Late Paleoproterozoic mantle plume events of Central and Southeastern Brazil. Journal of Geodynamics, 39(3), 197−208. https://doi.org/10.1016/j.jog.2004.10.003

Condie K.C. 1981. Archean Greenstone Belts. Developments in Precambrian Geology, Amsterdã, Elsevier, 3. 434 p.

Costa M.T., Branco J.J.R. 1961. Introdução. In: Branco J.J.J.R. (ed). Roteiro para excursão Belo Horizonte-Brasília. Belo Horizonte, SBG, Congresso Brasileiro de Geologia, 15, p. 1–119.

Costa M.T., Romano A.W. 1976. Mapa Geológico do Estado de Minas Gerais, Escala 1:1.000.000. Belo Horizote, CPRM. Available online at: https://rigeo.cprm.gov.br/handle/doc/5016 / (accessed on 10 March 2023).

CPRM - Serviço Geológico do Brasil. 2019. Afloramentos na região da Faixa Pará de Minas - Pitangui. Arquivos XYZ. GeoSGB: base de dados: afloramentos. Belo Horizonte, CPRM. Available online at: https://geosgb.cprm.gov.br / (accessed on 07 July 2022).

Cubas C.A.C. 2019. Análise de fácies e ambientes deposicionais de uma sucessão sedimentar paleoproterozoica do Noroeste do Quadrilátero Ferrífero, região de Pitangui. Scientific Initiation Report, Universidade Federal de Ouro Preto, Ouro Preto, 16 p.

Dardenne M.A. 1978. Síntese sobre a estratigrafia do Grupo Bambuí no Brasil Central. In: Congresso Brasileiro de Geologia, 30, 2, 597–610. Available online at: http://www.sbgeo.org.br/home/pages/44 / (accessed on 10 March 2023).

Dardenne M.A. 1981. Os grupos Paranoá e Bambuí na Faixa Dobrada Brasília. In: Simpósio sobre o Cráton São Francisco, 140–157. Available online at: http://www.sbgeo.org.br/home/pages/44 / (accessed on 10 March 2023).

Di Salvio L.P.P., Silva R.N., Brito D.C., Marinho M.S., Féboli W.L., Dreher A., Magalhães J.R. 2017. Geocronologia da sequência basal do Greenstone Belt Rio das Velhas no sinclinório Pitangui, NW do Quadrilátero Ferrífero. In: Simpósio de Geologia do Sudeste, 14. Available online at: http://www.sbgeo.org.br/home/pages/44 / (accessed on 10 March 2023).

Di Salvio L.P., Silva R.N., Matinho M.S., Lombello J.C. 2019a. Mapa geológico e de recursos minerais - Folha SE.23-Z-C-IV-1-NO, Escala 1:25.000. Projeto ARIM, Belo Horizonte, CPRM. Available online at: https://rigeo.cprm.gov.br/handle/doc/19409 / (accessed on 24 January 2023).

Di Salvio L.P., Silva R.N., Matinho M.S., Lombello J.C. 2019b. Mapa geológico e de recursos minerais - Folha SE.23-Z-C-IV-1-SO, Escala 1:25.000. Projeto ARIM, Belo Horizonte, CPRM. Available online at: https://rigeo.cprm.gov.br/handle/doc/19387 / (accessed on 24 January 2023).

Di Salvio L.P., Silva R.N., Matinho M.S., Lombello J.C. 2019c. Mapa geológico e de recursos minerais - Folha SE.23-Z-C-IV-3-NO, Escala 1:25.000. Projeto ARIM, Belo Horizonte, CPRM. Available online at: https://rigeo.cprm.gov.br/handle/doc/19405 / (accessed on 24 January 2023).

Dopico C.I.M., Lana C., Moreira H.S., Cassino L.F., Alkmim F.F. 2017. U–Pb ages and Hf-isotope data of detrital zircons from the late Neoarchean-Paleoproterozoic Minas Basin, SE Brazil. Precambrian Research, 291, 143–161. https://doi.org/10.1016/j.precamres.2017.01.026

Dorr II J.V.N. 1969. Physiographic, stratigraphic and structural development of the Quadrilátero Ferrífero, Minas Gerais, Brazil. Geological Survey Professional Paper, 641-A., Washington, U.S. Government Printing Office, 110 p. Available online at: https://doi.org/10.3133/pp641A / (accessed on 10 March 2023).

DNPM - Departamento Nacional de Produção Mineral. 2010. Anuário Mineral Brasileiro. Brasília, DNPM. Available online at: https://www.gov.br/anm/pt-br/centrais-de-conteudo/publicacoes/serie-estatisticas-e-economia-mineral/anuario-mineral/anuario-mineral-brasileiro / (accessed on 10 March 2023).

Eyles C.H., Eyles N. 2000. Subaqueous mass flow origin for Lower Permian diamictites and associated facies of the Grant Group, Barbwire Terrace, Canning Basin, Western Australia. Sedimentology, 47(2), 343–356. https://doi.org/10.1046/j.1365-3091.2000.00295.x

Eriksson K.A., Krapez B., Fralick P.W. 1994. Sedimentology of Archean greenstone belts: signatures of tectonic evolution. Earth-Science Reviews, 37(1-2), 1-88. https://doi.org/10.1016/0012-8252(94)90025-6

Eriksson P.G., Altermann W., Nelson D.R., Mueller W.U., Catuneanu O. 2004. Sedimentation through time. In: The Precambrian Earth: Tempos and Events. Developments in Precambrian Geology, 12, 593-680.

Fabricio-Silva W., Rosière C.A., Bühn B. 2019. The shear zone-related gold mineralization at the Turmalina deposit, Quadrilátero Ferrífero, Brazil: Structural evolution and the two stages of mineralization. Mineralium Deposita, 54, 347–368. https://doi.org/10.1007/s00126-018-0811-7

Fabrício-Silva W., Frimmel H.E., Shutesky M.E., Rosière C.A., Massucatto A. 2021. Temperature-Controlled Ore Evolution in Orogenic Gold Systems Related to Synchronous Granitic Magmatism: An Example from The Iron Quadrangle Province, Brazil. Economic Geology, 116 (4), 937–962. http://doi.org/10.5382/econgeo.4814

Farina F., Albert C., Lana C. 2015. The Neoarchean transition between medium - and high-K granitoids: clues from the Southern São Francisco Cráton (Brazil). Precambrian Research, 266, 375-394. https://doi.org/10.1016/j.precamres.2015.05.038

Farina F., Albert C., Martínez-Dopico C., Aguilar-Gil C., Moreira H., Hippert J.P., Cutts K., Alkimin F.F., Lana C. 2016. The Archean–Paleoproterozoic evolution of the Quadrilátero Ferrífero (Brasil): Current models and open questions. Journal of South American Earth Sciences, 68, 4–21. https://doi.org/10.1016/j.jsames.2015.10.015

Féboli W.L., Marinho M.S. 2019a. Mapa geológico e de recursos minerais - Folha SE.23-Z-C-IV-2-NO, Escala 1:25.000. Projeto ARIM, Belo Horizonte, CPRM. Available online at: https://rigeo.cprm.gov.br/handle/doc/19403 / (accessed on 24 January 2023).

Féboli W.L., Marinho M.S. 2019b. Mapa geológico e de recursos minerais - Folha SE.23-Z-C-IV-4-NO, Escala 1:25.000. Projeto ARIM, Belo Horizonte, CPRM. Available online at: https://rigeo.cprm.gov.br/handle/doc/19168 / (accessed on 24 January 2023).

Féboli W.L., Marinho M.S., Lombello J.C. 2019. Mapa geológico e de recursos minerais - Folha SE.23-Z-C-IV-2-SO, Escala 1:25.000. Projeto ARIM, Belo Horizonte, CPRM. Available online at: https://rigeo.cprm.gov.br/handle/doc/19378 / (accessed on 24 January 2023).

Frizzo C., Takai V., Scarpelli W. 1991. Auriferous mineralization at Pitangui, Minas Gerais. In: Ladeira E.A. Brazil Gold'91. Rotterdam, Balkema, p. 579-583.

Grossi-Sad J.H. 1968. Esboço Geológico do Estado de Minas Gerais, Escala 1:1.000.000. Belo Horizonte, Geosol.

Hartmann L.A., Endo I., Suita M.T.F., Santos J.O.S., Frantz J.C., Carneiro M.A., McNaughton N.J., Barley M.E. 2006. Provenance and age delimitation of Quadrilátero Ferrífero sandstones based on zircon U-Pb isotopes. Journal of South American Earth Sciences, 20(4), 273–285. https://doi.org/10.1016/j.jsames.2005.07.015

Koglin N., Zeh A., Cabral A.R., Gomes Jr. A.A.S., Corrêa Neto A.V., Brunetto W.J., Galbiatti H. 2014. Depositional age and sediment source of the auriferous Moeda Formation, Quadrilátero Ferrífero of Minas Gerais Brazil: new constraints from U-Pb–Hf isotopes in zircon and xenotime. Precambrian Research, 255, 96–108. https://doi.org/10.1016/j.precamres.2014.09.010

Kuchenbecker M., Babinski M., Pedrosa-Soares A.C., Costa R.D., Lopes-Silva L., Pimenta F. 2013. Proveniência e análise sedimentar da porção basal do Grupo Bambuí em Arcos (MG). Geologia USP, Série Científica, 13(4), 49–61. https://doi.org/10.5327/Z1519-874X201300040003

Ladeira E.A. 1981. Primeiras lavas com almofadas ("pillow") encontradas no Supergrupo Rio das Velhas, de idade arqueana, no Quadrilátero Ferrífero e no Distrito de Pitangui, Minas Gerais. Ciências da Terra, 1(1), 12-14.

Lana C., Alkimin F.F., Armstrong R., Scholz R., Romano R., Nalini H.A. 2013. The ancestry and magmatic evolution of Archaean TTG rocks of the Quadrilátero Ferrífero province, southeast Brazil. Precambrian Research, 231, 157-173. https://doi.org/10.1016/j.precamres.2013.03.008

Lobato L.M., Ribeiro-Rodrigues L.C., Vieira F.W.R. 2001. Brazil's premier gold province. Part II: geology and genesis of gold deposits in the Archean Rio das Velhas greenstone belt, Quadrilátero Ferrífero. Mineralium Deposita, 36, 249-277. https://doi.org/10.1007/s001260100180

Lombello J.C., Marinho M.S. 2019a. Mapa geológico e de recursos minerais - Folha SE.23-Z-C-IV-2-SE, Escala 1:25.000. Projeto ARIM, Belo Horizonte, CPRM. Available online at: https://rigeo.cprm.gov.br/handle/doc/21254 / (accessed on 24 January 2023).

Lombello J.C., Marinho M.S. 2019b. Mapa geológico e de recursos minerais - Folha SE.23-Z-C-IV-4-NE, Escala 1:25.000. Projeto ARIM, Belo Horizonte, CPRM. A Available online at: https://rigeo.cprm.gov.br/handle/doc/21253 / (accessed on 24 January 2023).

Lombello J.C., Marinho M.S. 2019c. Mapa geológico e de recursos minerais - Folha SE.23-Z-C-IV-4-SE, Escala 1:25.000. Projeto ARIM, Belo Horizonte, CPRM. Available online at: https://rigeo.cprm.gov.br/handle/doc/21252 / (accessed on 24 January 2023).

Luz A.B., Tomedi P., Martins R. 2005. Agalmatolito. In: Rochas & minerais industriais: usos e especificações. Rio de Janeiro, CETEM, MCT, 3, 73-84.

Machado N., Schrank A., Noce C.M., Gauthier G. 1996. Ages of detrital zircon from Archean-Paleoproterozoic sequences: Implications for Greenstone Belt setting and evolution of a Transamazonian foreland basin in Quadrilátero Ferrífero, southeast Brazil. Earth and Planetary Science Letters, 141(1-4), 259-276. https://doi.org/10.1016/0012-821X(96)00054-4

Magalhães J.R., Marinho M.S., Féboli W.L., Silva R.N., Brito D.C., Salvio L.P.P., Rodrigues J.B. 2019. Magmatismo granítico meso-a neoarqueano associado ao Greenstone Belt Rio das Velhas no sinclinório de Pitangui, Quadrilátero Ferrífero – MG. In: Simpósio de Geologia do Sudeste, 16. Available online at: http://www.sbgeo.org.br/home/pages/44 / (accessed on 09 March 2023).

Marinho M.S., Di Sálvio L.P.P., Brito D.C., Silva R.N., Féboli W.L., Dreher A.M., Silva M.A. 2017. O mapeamento geológico 1:25.000 no sinclinório de Pitangui, noroeste do Quadrilátero Ferrífero – resultados preliminares. In: Simpósio de Geologia do Sudeste, 14. Available online at: http://www.sbgeo.org.br/home/pages/44 / (accessed on 9 March 2023).

Marinho M.S., Silva M.A.D., Lombello J.C., Di Salvio L.P.P., Silva R.N., Féboli W.L., Brito D.C. 2019. Mapa geológico e de recursos minerais integrado: área de relevante interesse mineral, ARIM, Quadrilátero

Ferrífero, faixa Pará de Minas-Pitangui, Escala 1:75.000. Belo Horizonte, CPRM. Available online at: https://rigeo.cprm.gov.br/handle/doc/19393 / (accessed on 24 January 2023).

Martins M., Lemos V.B. 2007. Análise estratigráfica das sequências neoproterozóicas da Bacia do São Francisco. Revista Brasileira de Geociências, 37(4), 156–167. Available online at: https://ppegeo.igc.usp.br/index.php/rbg/article/view/9231/0 / (accessed on 9 March 2023).

Martins L., Lana C., Mazoz A., Novo T. 2022. Chemical-Abrasion U-Pb zircon geochronology reveals 150 Myr of partial melting events in the Archean crust of the São Francisco Craton. Geoscience Frontiers, 13(5), 101289. https://doi.org/10.1016/j.gsf.2021.101289

Matos C.A., Amorim P.H., Marinho M.S., Marangoni Y.R., Araújo J.C.S., Oliveira R.G., Lombello J.C. 2022. Gravity surveys and 3D integrated model with magnetic and geological data of the granite-greenstone terrane in Pitangui Synclinorium, NW of the Quadrilátero Ferrífero (MG, Brazil). Journal of South American Earth Sciences, 116, 103828. https://doi.org/10.1016/j.jsames.2022.103828

Melo-Silva P., Amaral W.S., Oliveira E.P. 2020. Geochronological evolution of the Pitangui greenstone belt, Southern São Francisco Craton, Brazil: constraints from U-Pb zircon age, geochemistry and field relationships. Journal of South America Earth Sciences, 99, 102380. https://doi.org/10.1016/j.jsames.2019.102380

Moreira D.S., Uhlein A., Dussin I.A., Uhlein G.J., Misuzaki A.M.P. 2020. A Cambrian age for the upper Bambuí Group, Brazil, supported by the first U-Pb dating of volcaniclastic bed. Journal of South American Earth Sciences, 99, 102503. https://doi.org/10.1016/j.jsames.2020.102503

Moreira H., Lana C., Naline Jr. H.A. 2016. The detrital zircon record of an Archaean convergent basin in the Southern São Francisco Craton, Brazil. Precambrian Research, 275, 84-99. http://dx.doi.org/10.1016/j.precamres.2015.12.015

Noce C.M. 1995. Geocronologia dos eventos magmáticos, sedimentares e metamórficos na região do Quadrilátero Ferrífero, Minas Gerais. PhD Thesis, Instituto de Geociências, Universidade de São Paulo, São Paulo, 129p.

Noce C.M., Teixeira W., Machado N. 1997. Geoquímica dos gnaisses TTG e granitóides neoarqueanos do Complexo Belo Horizonte, Quadrilátero Ferrífero, Minas Gerais. Revista Brasileira Geociências, 27(1), 25-32. https://doi.org/10.25249/0375-7536.19972532

Noce C.M., Machado N., Teixeira W. 1998. U/Pb Geochronology of gneisses and granitoids in the Quadrilátero Ferrífero (Southern São Francisco Craton): age constraints for Archean and Paleoproterozoic magmatism and metamorphism. Revista Brasileira de Geociências, 28, 95-102. http://doi.org/10.25249/0375-7536.199895102

Paula-Santos G.M., Babinski M., Kuchenbecker M., Caetano-Filho S., Trindade R.I., Pedrosa-Soares A.C. 2015. New evidence of an Ediacaran age for the Bambuí Group in southern São Francisco craton (eastern Brazil) from zircon U–Pb data and isotope chemostratigraphy. Gondwana Research, 28(2), 702-720. https://doi.org/10.1016/j.gr.2014.07.012

Reis H.L.S., Suss J.F., Fonseca R.C.S., Alkmim F.F. 2017. Ediacaran forebulge grabens of the southern São Francisco basin, SE Brazil: Craton interior dynamics during West Gondwana assembly. Precambrian Research, 302, 150–170. https://doi.org/10.1016/j.precamres.2017.09.023

Richter P., Lacerda G.M., Hagen D., Bosum W., Paulsen S., Souza A.A., Bruno E.M., Gomes N.S., Mollat H., Barthel F., Glatte W., Saam H., Zimmermann K., Kossmehl H. 1975. Relatório de reconhecimento geológico-geoquímico Pitangui-Papagaios-Pequi, MG. Belo Horizonte, CPRM, 80 p. Available online at: https://rigeo.cprm.gov.br/handle/doc/7152 / (accessed on 10 March 2023).

Rocha-Campos A.C., Brito-Neves B.B., Babinski M., Santos P.R., Oliveira S.M.B., Romano A.W. 2011. Moema laminites: a newly recognized Neoproterozoic (?) glaciogenic unit, São Francisco Basin, Brazil. In: Arnaud E., Halverson G.P., Shields-Zhou G. (eds.), The geological record of Neoproterozoic glaciations. Memoir, 36, London, Geological Society, p. 535–540.

Romano A.W., Carmo J.C.C. 1992. Estratigrafia e alteração hidrotermal das rochas do supergrupo Rio das Velhas no sinclinório de Pitangui-Pequi, Minas Gerais. Revista da Escola de Minas, 45(1-2), 115-117.

Romano A.W., Knauer L.G. 2003. Evidências da glaciação neoproterozóica na base do Grupo Bambuí - região de Onça do Pitangui - Minas Gerais. In: Simpósio de Geologia de Minas Gerais, 1, 27.

Romano A. 2007. Nota explicativa da Folha Pará de Minas (SE.23-Z-C-IV), 1:100.000. Programa Geologia do Brasil, Brasília, CPRM, UFMG, 72 p. Available online at: https://rigeo.cprm.gov.br/xmlui/handle/doc/10765 / (accessed on 9 March 2023).

Romano A.W. 1989. Évolution tectonique de la région Nord-Ouest du Quadrilatère Ferrifère - Minas Gerais-Brésil. PhD Thesis, CRPG-CNRS, Université de Nancy I, Vandoeuvre-lès-Nancy, France, 259 p.

Romano A.W., Paiva C.T. 1997. Evolução de eventos tectônicos, metamórficos e de alteração hidrotermal ao longo de uma zona de cisalhamento: exemplo do Lineamento Pitangui, parte meridional do Craton do São Francisco, MG. In Simpósio Nacional de Estudos Tectônicos, 6, 1, 21-22.

Romano R., Lana C., Alkmin F.F., Stevens G., Armstrong R. 2013. Stabilization of the Southern portion of the São Francisco Craton, SE Brazil, through a long-lived period of potassic magmatism. Precambrian Research, 224, 143-159. https://doi.org/10.1016/j.precamres.2012.09.002

Rossi A.V., Danderfer Filho A., Bersan S.M., Kelmer L.R., Tavares T.D., Lana C. 2020. Stratigraphic, isotopic, and geochronological record of a superposed pro-foreland basin in the eastern São Francisco craton during west Gondwana amalgamation. Journal of South American Earth Sciences, 97, 102406. https://doi.org/10.1016/j.jsames.2019.102406

Rossignol C., Lana C., Alkmim F.F. 2020. Geodynamic evolution of the Minas Basin, southern São Francisco Craton (Brazil), during the early Paleoproterozoic: Climate or tectonic? Journal of South American Earth Sciences, 101, 102628. https://doi.org/10.1016/j.jsames.2020.102628

Sampaio P.A.B. 2019. Litogeoquímica e petrografia das rochas encaixantes e da mineralização do depósito Aurífero Pontal, Greenstone Belt Pitangui, Conceição do Pará (MG). Graduation work, Universidade Federal do Rio de Janeiro, Rio de Janeiro, 81 p.

Scholl W.U. 1976. Sedimentologia e Geoquímica do Grupo Bambuí na parte sudeste da Bacia do São Francisco. In: Congresso Brasileiro de Geologia, 29, 2, 207. Available online at: http://www.sbgeo.org.br/home/pages/44 / (accessed on 10 March 2023).

Schrank A., Machado N. 1996. Idades U-Pb em monazitas e zircões das minas de Morro Velho e Passagem de Mariana - Quadrilátero Ferrífero (MG). In: Congresso Brasileiro de Geologia, 39, 6, 470-472. Available online at: http://www.sbgeo.org.br/home/pages/44 / (accessed on 10 March 2023).

Secco P.R. 2009. Caracterização dos tipos de agalmatolito da Serra dos Ferreiras, Onça do Pitangui-MG. MSc Dissertation, Instituto de Geociências, Universidade Federal de Minas Gerais, Belo Horizonte, 101 p. Available online at: http://hdl.handle.net/1843/MPBB-7VHQLP / (accessed on 10 March 2023).

Silva A.M., Chemale F.Jr., Kuyumjian R.M., Heaman L. 1995. Mafic dyke swarms of Quadrilatero Ferrifero and Southern Espinhaço, Minas Gerais, Brazil. Revista Brasileira de Geociências, 25(2), 124–137. Available online at: https://ppegeo.igc.usp.br/index.php/rbg/issue/view/1111 / (accessed on 10 March 2023).

Silva M.A., Pinto C.P., Pinheiro M.A.P., Marinho M.S., Lombello J.C., Pinho, J.M.M.P., Goulart L.E.A., Magalhães J.R. 2020. Mapa Geológico do Estado de Minas Gerais, Escala 1:1.000.000. Projeto Geologia do Estado de Minas Gerais, Belo Horizonte, CPRM. Available online at: https://rigeo.cprm.gov.br/xmlui/handle/doc/21828 / (accessed on 24 January 2023).

Straub K.M., Duller R.A., Foreman B.Z., Hajek, E.A. 2020. Buffered, incomplete and shredded: The challenges of reading an imperfect stratigraphic record. Journal of Geophysical Research: Earth Surface, 125(3). https://doi.org/10.1029/2019JF005079

Tavares T.D., Martins M.S., Alkmim F.F., Lana C. 2020. Detrital zircons from the Upper Três Marias Formation, São Francisco basin, SE Brazil: record of foreland deposition during the Cambrian? Journal of South American Earth Sciences, 97, 102395. https://doi.org/10.1016/j.jsames.2019.102395

Teixeira W., Ávila C.A., Dussin I.A., Corrêa Neto A.C., Bongiolo E.M., Santos J.O., Barbosa N.S. 2015. A juvenile accretion episode (2.35–2.32 Ga) in the Mineiro belt and its role to the Minas accretionary orogeny: Zircon U–Pb–Hf and geochemical evidences. Precambrian Research, 256, 148-169. https://doi.org/10.1016/j.precamres.2014.11.009

Teixeira N.A., Kuyumjian R.M. 1991. The Mateus Leme-Pitangui hidrothermal zone: Do They represent a fossil hot spring system in the Rio das Velhas greenstone belt, Central Brazil? In: Ladeira E.A. Brazil Gold`91. Rotterdam, Balkema, p. 171-177.

Tucker M.E. 2014. Rochas Sedimentares: guia geológico de campo. 4th ed. Porto Alegre, Bookman, 324 p.

Tuller M.P, Ribeiro J.H, Signorelli N., Féboli W.L, Pinho J.M.M. 2010. Projeto Sete Lagoas – Abaeté: estado de Minas Gerais. Belo

Horizonte, CPRM, 160 p. Available online at: https://rigeo.cprm.gov.br/handle/doc/11135 / (accessed on 10 March 2023).

Uhlein G.J., Carvalho J.F.M.G., Uhlein A., Caxito F.A., Halverson G.P., Sial A.N. 2012. Estratigrafia e sedimentologia da Formação Carrancas, Grupo Bambuí, nas regiões de Belo Horizonte e Pitangui, MG. Geonomos, 20(2), 79-97. https://doi.org/ 10.18285/geonomos.v2i20.250

Uhlein G.J. 2014. Proveniência sedimentar e estratigrafia das formações Carrancas e Lagoa Formosa e a evolução do Grupo Bambuí (635–570 Ma) em Minas Gerais. MSc Thesis, Universidade Federal de Minas Gerais, Belo Horizonte, 147p. Available online at: http://hdl.handle.net/1843/IGCC-9NDGEK / (accessed on 10 March 2023).

Uhlein G.J., Uhlein A., Halverson G.P., Stevenson R., Caxito F.A., Cox G.M., Carvalho J.F.M.G. 2016. The Carrancas Formation, Bambuí Group: a record of pre-Marinoan sedimentation on the southern São Francisco craton, Brazil. Journal of South America Earth Sciences, 71, 1–16. https://doi.org/10.1016/j.jsames.2016.06.009

Verma S.K., Oliveira E.P., Silva P.M., Moreno J.A., Amaral W.S. 2017. Geochemistry of komatiites and basalts from the Rio das Velhas and Pitangui greenstone belts, São Francisco Craton, Brazil: implications for the origin, evolution, and tectonic setting. Lithos, 284–285, 560–577. https://doi.org/10.1016/j.lithos.2017.04.024

Vieira L.C., Almeida R.P., Trindade R.I.F., Nogueira A.C.R., Janikian L. 2007. A Formação Sete Lagoas em sua área tipo: Fácies estratigrafia e sistemas deposicionais. Revista Brasileira de Geociências 37(4), 168-181. Available online at: https://ppegeo.igc.usp.br/index.php/rbg/issue/view/839 / (accessed on 10 March 2023).

Vieira L.C., Nédélec A., Fabre S., Trindade R.I.F., Almeida R.P. 2015. Aragonite crystal fans in Neoproterozoic cap carbonates: a case study from Brazil and implications for the post-Snowball Earth coastal environment. Journal of Sedimentary Research, 85(3), 285–300. https://doi.org/10.2110/jsr.2015.21

Warren L.V., Quaglio F., Riccomini C., Simoes M.G., Poire D.G., Strikis N.M., Anelli L.E., Strikis P.C. 2014. The puzzle assembled: Ediacaran guide fossil Cloudina reveals an old proto-Gondwana seaway. Geology, 42(5), 391–394. https://doi.org/10.1130/G35304.1